



MASTER THESIS

# PEAK TIBIAL ACCELERATION AS AN INDICATOR OF TIBIAL BONE LOAD DURING RUNNING

X.J. TER WENDEL

DEPARTMENT OF BIOMEDICAL SIGNALS AND SYSTEMS

FACULTY OF ELECTRICAL ENGINEERING MATHEMATICS  
AND COMPUTER SCIENCE

EXAMINATION COMMITTEE

M.A. Zandbergen, MSc

ir. R.P. van Middelaar

dr. E.H.F. van Asseldonk

dr. J. Reenalda

prof. dr. ir. P.H. Veltink

18-01-2022

UNIVERSITY OF TWENTE.



# Peak Tibial Acceleration As An Indicator of Tibial Bone Load During Running

Xanthe J. ter Wengel<sup>1,2</sup>, Marit A. Zandbergen<sup>2,1</sup>, Robbert P. van Middelaar<sup>1</sup>, Edwin H.F. van Asseldonk<sup>3</sup>, Jasper Reenalda<sup>1,2</sup>, and Peter H. Veltink<sup>1</sup>

<sup>1</sup> *Department of Biomedical Signals and Systems, Faculty of Electrical Engineering Mathematics and Computer Science, University of Twente, Enschede, The Netherlands*

<sup>2</sup> *Roessingh Research and Development, Enschede, The Netherlands*

<sup>3</sup> *Department of Biomechanical Engineering, Faculty of Engineering Technology, University of Twente, Enschede, The Netherlands*

## Author Note

This paper was written for the thesis of the first author to obtain the title Master of Science in Biomedical Engineering at the University of Twente. Final submission was on 18 January 2022.



### Samenvatting

Stressfracturen zijn een veelvoorkomende hardloopleesure en treden vaak op aan het scheenbeen. Deze blessure ontstaat door herhaalde belasting op het bot tijdens hardlopen. De piekversnelling van het onderbeen wordt vaak gebruikt als maat voor de krachten die werken op het onderbeen, maar een validatie hiervan ontbreekt. Dit onderzoek heeft gekeken naar de correlaties tussen de versnelling van het onderbeen en de krachten op het bot tijdens hardlopen over verschillende snelheden, stapfrequenties en versnellingsmeterlocaties. Negen getrainde hardlopers hebben een protocol uitgevoerd op een loopband, wat bestond uit negen delen. De hardlopers liepen hierbij op 10, 12 en 14 km/h voor eigen stapfrequentie, tien procent lager dan eigen stapfrequentie en tien procent hoger dan eigen stapfrequentie. De correlaties tussen de piekversnelling van het onderbeen en de krachten die werkten op het bot waren voornamelijk afwezig. Deze resultaten laten zien dat gebruik van de piekversnelling van het onderbeen als een maat voor de krachten die werken op het onderbeen wellicht ongeschikt is. Een toename van de piekversnelling van het onderbeen betekent dus niet direct ook een hogere belasting op het scheenbeenbot of een hoger risico op het ontstaan van een stressfractuur. Er is echter meer onderzoek nodig naar de validiteit van de gebruikte maat van de krachten die werken op het onderbeen. Verder onderzoek zou zich daarnaast kunnen richten op het berekenen van kinetische gegevens uit inertiaële sensoren. Dit onderzoek draagt bij aan bestaand onderzoek naar het gebruik van de piekversnelling van het onderbeen als indicator voor botbelasting van het scheenbeen tijdens hardlopen.



### Abstract

Stress fractures are a common running injury which often occur at the tibia and are the result of repeated loading on the bone. Peak tibial acceleration (PTA) has often been used as an indicator of tibial bone loading, but a validation of this metric is lacking. This study compared agreement between PTA and tibial bone loading across different speeds, step frequencies (SFs) and accelerometer locations. Nine trained runners performed a protocol on a treadmill consisting of running nine trials at 10, 12 and 14 km/h at preferred SF, 10% above preferred SF and 10% below preferred SF. Correlations between PTA and tibial bone loading were mostly absent. The findings indicate that the use of PTA as an indicator of the forces acting on the tibia might not be appropriate. An increase in PTA should thus not directly be assumed to also mean an increase in tibial bone loading or a higher risk on an overuse injury at the tibia. However, more research is needed on the validity of the used tibial bone loading metric. Further research should also focus on calculating kinetics from inertial measurement unit data. This research has added to the existing research on using PTA as an indicator of tibial bone loading.

*Key words:* peak tibial acceleration, running, tibial bone load, inertial measurement unit



**List of Abbreviations**

|                         |                                   |
|-------------------------|-----------------------------------|
| $\beta$                 | 3D angle between tibia and GRF    |
| BW                      | Body weights                      |
| COM                     | Center of mass                    |
| COP                     | Center of pressure                |
| $F_{\text{tibia, max}}$ | Maximal tibial compression force  |
| FM                      | Free moment                       |
| GRF                     | Ground reaction force             |
| GRM                     | Ground reaction moment            |
| IC                      | Initial contact                   |
| IMU                     | Inertial measurement unit         |
| $M_{\text{ankle}}$      | Ankle moment in sagittal plane    |
| PTA                     | Peak tibial acceleration          |
| $r$                     | Pearson's correlation coefficient |
| $r_{\text{tendon}}$     | Achilles tendon moment arm        |
| ROM                     | Range of motion                   |
| SD                      | Standard deviation                |
| SF                      | Step frequency                    |



## Introduction

Running is a sport associated with a high incidence of injuries [1]. Most of these injuries occur at the lower extremity and are the result of overuse. An example of such an injury is a stress fracture, often occurring at the tibia [2–5]. The total loading on the tibia during running is the sum of the ground reaction force (GRF) and local muscle forces [6,7]. At the distal tibia, the total force can be up to 8-9 times body weights during (BW) running [6,8]. Due to this high loading on the bone during running, microdamage occurs. This microdamage occurs because the bone is not able to remodel the damage of the applied loads. When this goes on for a prolonged period of time, microdamage accumulates and weakens the bone. Eventually, if the bone does not get enough time to repair this damage, the bone cracks and a stress fracture occurs [9,10]. If it would be possible to estimate the forces acting on the tibia during running, it would not only help understand when stress fractures occur, but also on how to potentially prevent them.

Various studies have been conducted to quantify the loading on the tibia, which in this study is defined as the total longitudinally compressive force acting on the distal end of the tibia, see also figure 1. Methods to measure this force include *in vivo* measurements and biomechanical modelling. However, these methods have some drawbacks. *In vivo* measurements require a surgical intervention to place a gauge or extensometer directly on the bone [11]. This makes it a highly invasive method and unsuitable for measuring a large group of runners. Biomechanical modelling can be divided into computational and analytical modelling, which need the collection of computed tomography images and kinetic data, respectively [6,12–15]. This can be time-consuming and costly, making it hard to implement for a large group of runners. It has, nevertheless, been found to produce results similar to *in vivo* measurements [16]. However, it is important here to realize that assumptions need to be made in biomechanical modelling with regards to the model parameters to come to a solution, which impacts the results [17].

The forces on the tibia bone can also be indirectly estimated with metrics based on the ground reaction force (GRF), or metrics based on the acceleration of the lower leg. GRF is defined as the force exerted by the ground on the foot when the foot makes contact with the ground and can be measured with a force plate [18]. A typical vertical GRF pattern for a rearfoot striker is displayed in figure 2. GRF metrics include impact peak (peak in vertical GRF within 15-50 ms after ground contact, A in figure 2), active peak (maximum peak in vertical GRF, B in figure 2) and loading rate (impact peak divided by time to reach active peak, A (active peak) divided by C (time to reach peak) in figure 2) [18–20]. The general assumption is that an increase in those metrics reflects an increase in the impact force and therefore an increase in the loading on the tibia bone. Besides, several studies have reported significant differences in GRF metrics between runners with a history of tibial stress fractures and runners without a history of tibial stress fractures [21].

Recently, Matijevich et al. have assessed the relationship between tibial bone loading metrics and aforementioned GRF metrics [19]. Across different speeds and slopes, correlations between GRF metrics and tibial bone loading metrics (maximal tibial compression force and tibial compression force impulse over stance) were compared. In general, moderate to weak correlations between these tibia bone loading metrics and GRF metrics were reported. An explanation for this lies in the relative contribution of the muscle forces, which compress the bones together, to the total force acting on the tibia. During running, the total force acting on tibia during the stance phase is a combination of the forces exerted by the plantar flexors around the ankle joint and the force exerted by GRF on the foot [6,19]. GRF is generally found to be

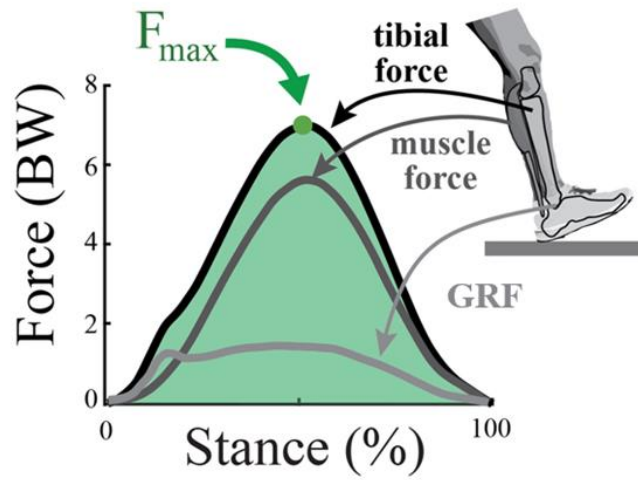


**Fig. 1** Tibial compression force over the stance phase, as the sum of the net force on the ankle (GRF) and the muscle force. Image obtained from Matijevich et al. (2020), figure 1, page 3 [22].

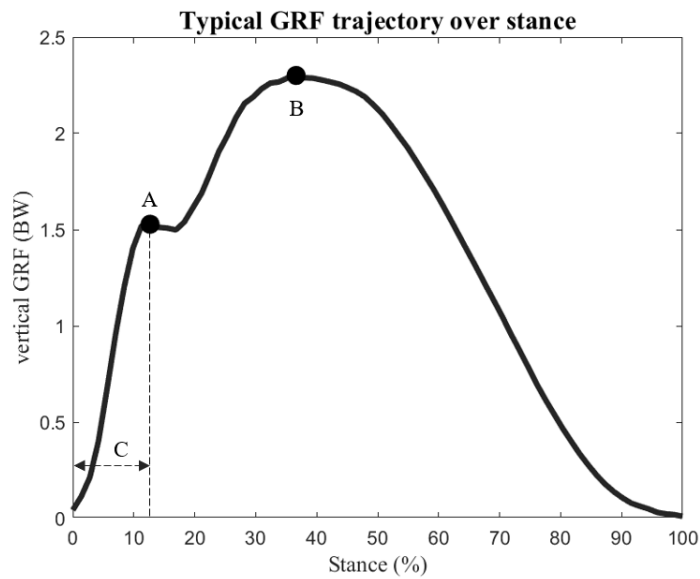


**Fig. 2** Typical vertical GRF trajectory over the stance time during running with impact peak (A), active peak (B) and loading rate (A/C) denoted.

equal to 2 BW, while plantar flexor force has been found to be equal to 5-6 BW (see also figure 1) [19]. The contribution of these plantar flexors is thus much higher compared to the contribution of GRF. Therefore, GRF only cannot explain the total force acting on the tibia. Dorsiflexors also contribute to the total force, but their contribution is quite low (0.5 BW). Besides, the force exerted by dorsiflexors only exists for certain parts of the stance phase [6,8].

Alternatively, the acceleration of the lower leg can be used. When the foot makes contact with the ground during running, a quick deceleration of part of the body occurs. This deceleration results in a shock wave that is transmitted through the whole body and can be measured as the impact acceleration [23]. Peak tibial acceleration (PTA) is defined as the impact acceleration measured at the tibia with a skin mounted accelerometer, which occurs shortly after initial contact (IC) [24]. Benefits of PTA include that it can easily and reliably be measured with portable equipment [24–29]. The general assumption is that PTA is reflective of the loading on the tibia caused by the foot hitting the ground. An increase in PTA would thus be indicative of an increase in the risk of tibial stress fractures [30]. However, it is assumed that the direct relationship between tibial bone loading and PTA is likely influenced by muscle forces, just as with GRF metrics [31].

Although previous papers have discussed how PTA is influenced by a number of factors, including speed, step frequency and placement of the accelerometer, research is lacking a study on the validity of PTA as the force acting on the tibia [23,31–35]. PTA is commonly used as an indicator of tibial bone loading because of its moderate to high correlations with GRF metrics, such as impact peak, active peak and loading rate [28,31,36,37]. But, as has been shown by Matijevich et al., those metrics might not be indicative of tibial bone loading [19]. Therefore, the validity of PTA as an indicator of tibial bone loading needs to be assessed.

This study aimed to answer the question: ‘What is the agreement between PTA and tibial bone loading?’. The agreement between PTA and tibial bone loading were assessed across different speeds, step frequencies (SFs) and accelerometer location on the tibia. Speed and SF were deemed appropriate conditions, as PTA has been shown to significantly change for changes in speed and SF [31–35]. Besides, an increase in running speed has been found to significantly increase muscle activity, so it is also expected that a change in speed will lead to a change in tibial bone loading [38]. The effect of SF on muscle activity during running is less profound, but muscle activity tends to decrease for increasing SF [39–41]. Therefore, it was hypothesized that PTA would be positively associated with speed and negatively associated with SF. It was also hypothesized that tibial bone loading would be positively associated with speed and negatively with SF, but that no strong agreement would be found between PTA and tibial bone loading for any of the conditions.

Earlier research has suggested that PTA is also influenced by the placement of the accelerometer on the shank [23]. The distance from the accelerometer to the ankle influences the angular acceleration of the tibia, which in turn influences the linear acceleration of the tibia [35]. Therefore, accelerometers placed closer to the knee underestimate PTA [31]. This was also assessed in this study by measuring PTA both proximally and distally. It was hypothesized that distal PTA would therefore be higher than proximal PTA, but that this would not lead to any differences in agreement between PTA and tibial bone loading.



## Methods

### Participants

Nine well-trained runners (5 men/4 women, age:  $31 \pm 9$  years, height:  $179.3 \pm 9.4$  cm, mass:  $75.0 \pm 18.7$  kg) who ran at least 15 km per week and were able to run at 14 km/h for 5 minutes were recruited. All runners reported no lower extremity injuries for the past six months. To avoid the effects of foot strike pattern on PTA and ankle moment, only rearfoot strikers were included [31,42]. Ethical approval was obtained from the local ethics committee<sup>1</sup>. Each runner gave written consent before participating in the study. The study was advertised through general e-mails sent to running clubs, social media posts and posters in running stores.

### Measurement devices

Each runner was equipped with an inertial motion capture system (240 Hz, MVN Link, Xsens, Enschede, The Netherlands). Sensors were placed on the sternum, sacrum, medio-lateral thighs (on iliotibial band), proximal medial surface of the tibia just below tibial tuberosity (where one axis was aligned with long axis of tibia), and the feet (in the shoes, over the mid-foot). This can be seen in figure 3. An additional sensor was placed just above the medial malleolus of the dominant leg. This distal sensor was aligned with the sensor on the proximal tibia and had thus also one axis aligned with the long axis of the tibia. Sensors were attached to the skin using double-sided tape and covered with an extra layer of adhesive tape. To keep the sensors on the lower legs firmly attached to the shin, participants wore slightly compressing sleeves.

The running protocol was performed on dual-belt instrumented treadmill (custom Y-mill, Motekforce Link, Culemborg, The Netherlands), located at the University of Twente (Enschede, The Netherlands). An embedded force plate in this treadmill collected 3D GRF and ground reaction moments (GRMs) at 2048 Hz. Heart rate (Garmin HRM2-SS CR2032, Olathe, KS, USA) and a modified Borg scale (asked at beginning and end of experiment) were used to ensure no fatigued state was reached within the experiment. Fatigue was measured because it can influence PTA [31]. During each trial, feet and lower legs were filmed with a high-speed camera (JVC GC-PX100BE, Yokohama, Japan) in order to assess foot strike pattern. SF was measured by means of a metronome (Tap BPM, Google Commerce Ltd, Dublin, Ireland).

### Experimental design

Relevant body dimensions (body height, hip height, hip width, knee height, ankle height, shoe length and shoe sole thickness) were obtained from every participant before the start of the running protocol. After a five-minute warm-up at a self-selected speed, calibration of the inertial motion capture system was performed and consisted of standing still for about five seconds and then walking back and forth for ten seconds on the ground in the laboratory, as prescribed by Xsens [43]. This was done for sensor to segment calibration. Runners then ran with their own shoes at three different speeds (10, 12 and 14 km/h) in a random order on the treadmill. Each speed had three trials of ninety seconds each, which consisted of running at preferred SF, running ten percent above preferred SF, and running ten percent below preferred SF. This can also be viewed in figure 4. Preferred SF was determined by an independent researcher who was trained in measuring SF in earlier pilot studies. An auditory metronome was then used to impose a SF of ten percent above and ten percent below preferred SF. Ten percent change in SF was chosen because previous research has established that a change of ten percent in SF is

---

<sup>1</sup> RP2021-117, Faculty of Electrical Engineering Mathematics and Computer Science, University of Twente, Enschede, The Netherlands



needed to see a difference in PTA [32,34]. To make sure runners were able to run at the imposed SFs as naturally as possible without any prior training, there was chosen to not go for any values higher than ten percent. After the last trial, one additional trial was measured where participants were instructed to stand in a neutral pose on the treadmill for ten seconds. This was later used for sensor-to-segment calibration. To minimize the risk of fatiguing a participant, each trial was followed by three minutes of rest. During each period of rest, participants were free to choose whether they wanted to stand still on the treadmill or walk at a maximum speed of five km/h.

### **Pre-processing**

The foot strike pattern of each runner for ten km/h preferred SF was assessed based on the obtained videos of the feet and the lower legs by two independent researchers. Only runners who had a rearfoot strike pattern were included. If the researchers disagreed on the foot strike pattern, an extra check was performed by looking at the vertical GRF pattern. A rearfoot strike pattern has an extra peak (impact peak) occurring in the GRF signal, before the main peak (see also figure 2) [44,45]. If an extra peak was detected, the foot strike pattern was assessed as a rearfoot, and the runner was included in the study. In case SF was not measured by accident, SF was determined from the acceleration data of the feet afterwards. If a change of less than five percent compared to preferred SF was observed during one of the trials, this trial was excluded from the study.

Xsens software (MVN Analyze, 2020.0.2, Xsens, Enschede, The Netherlands) and a custom code (MATLAB R2019b, MathWorks Inc., MA, USA) were used to obtain GRFs and GRMs from the force plate data and to obtain acceleration data. Orientation data (sensor) was obtained from the Xsens algorithm. A clockwise rotation of ninety degrees around the x-axis was applied to the force plate to express it in the same coordinate system as OpenSim, where the x-axis was forwards, the y-axis was upward, and the z-axis was medio-lateral (right-handed coordinate system). Center of pressure (COP) was then calculated based on GRF and GRM data, using the following formulas [46,47]:

$$\text{COP}_x = \frac{\text{GRM}_z}{\text{GRF}_y} \quad (1)$$

$$\text{COP}_z = -\frac{\text{GRM}_x}{\text{GRF}_y} \quad (2)$$

COP in y-direction was set to zero. After this, GRF, GRM and COP were filtered with a 20 Hz 4<sup>th</sup> order Butterworth recursive lowpass filter and down sampled to match the sampling frequency of the inertial motion capture system (240 Hz) [48]. Accelerations were filtered with a commonly used 60 Hz 4<sup>th</sup> order Butterworth recursive lowpass filter [31]. Force plate data of the treadmill and Xsens data were then synchronized by aligning the vertical acceleration of the pelvis with vertical GRF, using cross correlation (xcorr function in MATLAB). The first forty seconds of each trial were excluded to account for the effect of accelerating and adjusting to SF. After those forty seconds, data was set to begin at the first initial contact (IC) of the right foot. A vertical GRF threshold of 20 N was used to detect IC, similar to [49]. The first forty gait cycles of each trial were assessed for dominant leg.

### **Estimating tibial bone loading**

#### ***Inverse kinematics***

A musculoskeletal model was linearly scaled for every runner based on the height of the runner. In this study, the Rajagopal model was used. This is a full body, thirty-seven degrees of

freedom musculoskeletal model, which has been used before to study gait patterns during running [50–52]. Inverse kinematics were then computed according to the OpenSense workflow [53,54]. In the OpenSense workflow, orientation data from the sensors is used to compute kinematics. A more detailed description of this can be viewed in Appendix-I.

### *Inverse dynamics*

To perform inverse dynamics, the kinematics data first needed to be spatially aligned with the force plate data. Spatial synchronization of the force plate data and the kinematics was based on the assumption that during IC the center of mass (COM) of the calcaneus and the COP are equal for rearfoot strikers. This was done because the IMU-based model does not have a clearly defined fixed 3D positioning system. The offset between COM of the right calcaneus and COP during the first IC was calculated and COP was then adjusted for the whole trial based on this offset. COP and GRF were then used as an input for inverse dynamics in OpenSim. Free moment (FM) was set to zero. FM is the moment around an axis normal to the ground and is the result of the friction forces between the foot and the ground [55]. It is independent of the point of application of GRF. In general, FM during running is quite small, with maximum values ranging from 0.05 to 0.15 Nm/kg [55–57]. Because it was not possible to calculate FM in this study, it was set to zero, similarly to [58].

### *Calculating forces on tibia*

The ankle moment obtained from the inverse dynamics was used to calculate a metric for the total longitudinally compressive force acting on the distal end of the tibia, similar to [19]. It was assumed that the net force acting on the ankle was indicative of tibial bone loading. This force consisted of two components: an external force component ( $F_{\text{ext}}$ ) and an internal force component ( $F_{\text{int}}$ ). In this instance, the external force refers to the force exerted by the GRF on the tibia, and the internal force refers to the force exerted by the plantar flexor muscles on the tibia. The force of the dorsiflexors is assumed to be negligible, as the force is small and only existent for a small part of the stance phase [6,8].

GRF acts on the tibia at a certain angle,  $\beta$ . The force exerted by the plantar flexor muscles on the distal tibia can be approximated by dividing the sagittal ankle moment by the Achilles tendon moment arm, similar to [19]. This moment arm is the average moment arm of the plantar flexor muscles and is assumed constant at 5 cm, which is a typical Achilles tendon moment arm length [59–61]. This approximation to calculate the muscle force has been found to produce results similar to static optimization methods [62]. Hence, the total longitudinally compressive force acting on the distal end of the tibia ( $F_{\text{tibia}}$ , see also figure 1 and 5) can be expressed as:

$$F_{\text{tibia}}(t) = F_{\text{ext}}(t) + F_{\text{int}}(t) = |\text{GRF}(t)| * \cos(\beta(t)) + \frac{M_{\text{ankle}}(t)}{r_{\text{tendon}}} \quad (3)$$

Here,  $\beta$  is the norm of the 3D angle vector between tibia and GRF,  $M_{\text{ankle}}$  is the ankle moment in sagittal plane and  $r_{\text{tendon}}$  is the Achilles tendon moment arm (5 cm, [59–61]).  $\beta$  was calculated using the orientation of the lower leg and the orientation of the foot. The maximum longitudinally compressive tibia force ( $F_{\text{tibia, max}}$ ) was then calculated from this force and used as a metric for tibial bone loading.

### **Computing PTA**

The raw axial acceleration (including gravity) of the proximal and distal sensor on the tibia was filtered with a 60 Hz 4<sup>th</sup> order Butterworth recursive lowpass filter before, PTA was computed [31]. PTA was measured along the long axis of the tibia. The peaks in the

acceleration signal were located with the findpeaks function of MATLAB. Here, 'MinPeakDistance' was set to seventy-five percent of the distance between each step (expressed as  $1/SF$ ).

### **Statistical analyses**

To assess the influence of speed on the relation between tibial bone loading (expressed as  $F_{\text{tibia,max}}$ ) and PTA, their relation was computed for 10, 12 and 14 km/h at preferred SF for every runner. To assess the influence of SF on the agreement between tibial bone loading and PTA, their relation was computed for preferred SF, ten percent below preferred SF and ten percent above preferred SF at 12 km/h for every runner. To quantify the agreement between tibial bone loading and PTA in these relations, Pearson's correlation coefficient ( $r$ ) was computed for both relations. Here,  $r \geq 0.8$  indicated a strong correlation,  $0.5 \leq r < 0.8$  indicated a moderate correlation,  $0.3 \leq r < 0.5$  indicated a weak correlation and  $r < 0.3$  indicated a negligible correlation [63]. A generalized estimating equation (GEE) was used to test for significant correlations between PTA and maximal tibial compression force when looking at a group level. A repeated measures ANOVA was conducted to assess differences between distally measured PTA and proximally measured PTA across conditions. All statistical tests were performed in IBM SPSS 25.0 (IBM Corp, Armonk, NY, US). A significance level of  $\alpha = 0.05$  was used.

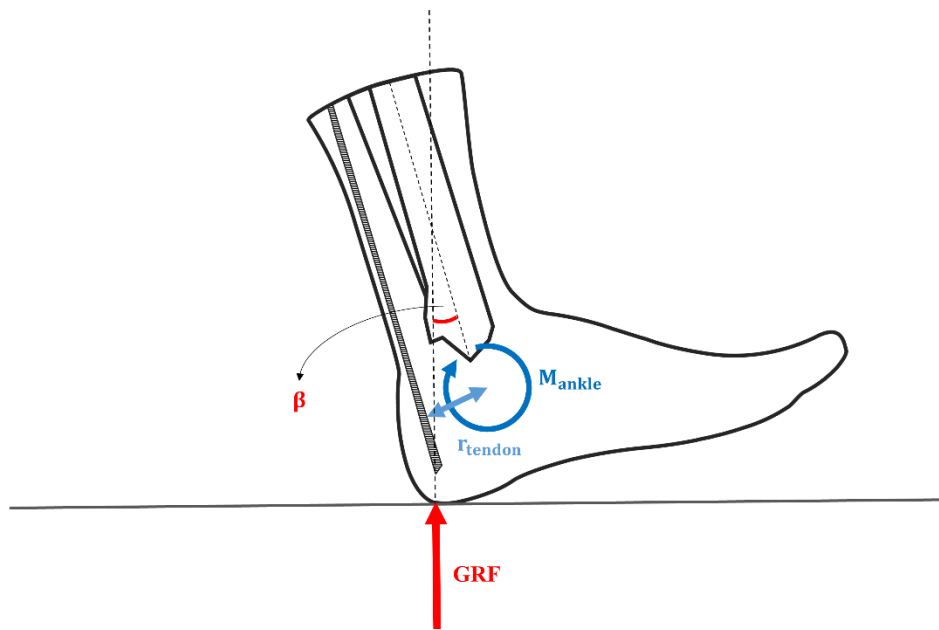


**Fig. 5** Schematic representation of parameters for calculating tibial bone loading force. The external force (depicted in red) represents the GRF which acts on an angle  $\beta$  at the tibia. The internal force represents the forces exerted by the muscles (depicted in blue) and is here calculated by dividing the sagittal ankle moment  $M_{ankle}$  by the Achilles tendon moment arm ( $r_{tendon}$ ).

## Results

At 12 km/h for preferred SF, the average proximal PTA was found to be equal to  $73.8 \pm 17.6 \text{ m/s}^2$  and the average distal PTA was found to be equal to  $76.0 \pm 14.0 \text{ m/s}^2$ . The average  $F_{\text{tibia,max}}$  was equal to  $21.5 \pm 3.2 \text{ BW}$  (see also figure 6-9 and table 3 in Appendix-II).  $F_{\text{tibia,max}}$  was expressed in BW in order to compare between runners. Trajectories of proximal tibial acceleration and  $F_{\text{tibia}}$  for runner 1 at 12 km/h with preferred SF over the stance phase are shown in figure 10.

Every runner showed a strong, positive correlation between proximal PTA and changes in speed ( $r > 0.7$  for all, see left side of table 4 in Appendix-III). One runner showed a moderate, positive correlation between proximal PTA and changes in SF ( $r = 0.5$ ), while four runners showed a negative, moderate to strong correlation between proximal PTA and changes in SF ( $r < -0.5$ , see right side of table 4 in Appendix-III). Correlations between distal PTA and changes in speed were similar ( $r > 0.7$ ). This was also the case for correlations between distal PTA and changes in SF, with the exception of two runners. Most runners showed a positive, moderate to strong correlation between  $F_{\text{tibia,max}}$  and changes in speed ( $r > 0.6$ ), with the exception of one who showed a negative strong correlation ( $r = -0.7$ ). Correlations between  $F_{\text{tibia,max}}$  and changes in SF tended to be negative.

### Agreement for changes in speed at preferred SF

Correlations between proximal PTA and  $F_{\text{tibia,max}}$  within runners for different speeds were absent in most runners (table 1, figures 11-16 in Appendix-IV). Found correlations ranged from weak to strong and both positive and negative correlations were found. A generalized estimation equation showed a significant correlation between proximal PTA and maximal tibial compression force for 10 and 14 km/h ( $p < 0.05$ ). Distally measured PTA was significantly higher than proximal PTA at 10 and 12 km/h, see figure 6. Correlations between distal PTA and  $F_{\text{tibia,max}}$  within runners were similar to correlations between proximal PTA and  $F_{\text{tibia,max}}$  (table 1). Two runners showed a weak correlation between distal PTA and  $F_{\text{tibia,max}}$ , while no correlation was reported between proximal PTA and  $F_{\text{tibia,max}}$  for these conditions. Three runners showed no correlation between distal PTA and  $F_{\text{tibia,max}}$ , while a weak correlation was reported between proximal PTA and  $F_{\text{tibia,max}}$  for these conditions. A generalized estimation equation showed a significant correlation between distal PTA and  $F_{\text{tibia,max}}$  for 12 km/h ( $p = 0.05$ ), but not for the other speeds.

### Agreement for changes in SF at 12 km/h

Correlations between proximal PTA and  $F_{\text{tibia,max}}$  for different SFs within runners were absent in most runners (table 2, see also figures 17-22 in Appendix-V). A moderate, negative correlation between proximal PTA and  $F_{\text{tibia,max}}$  was found for one runner. Some weak correlations were found and those tended to be negative. A generalized estimation equation showed a significant correlation between proximal PTA and  $F_{\text{tibia,max}}$  for preferred and ten percent above preferred SF ( $p < 0.01$ ). Distally measured PTA was significantly higher than proximally measured PTA at preferred SF and ten percent below preferred SF ( $p = 0.02$ , see figure 7). Correlations between distal PTA and  $F_{\text{tibia,max}}$  within runners tended to be similar to correlations between proximal PTA and  $F_{\text{tibia,max}}$  (table 2). Two runners showed weak correlations at preferred SF between distal PTA and  $F_{\text{tibia,max}}$ , while no correlations were found between proximal PTA and  $F_{\text{tibia,max}}$  at those conditions. A generalized estimation equation showed a significant correlation between distal PTA and  $F_{\text{tibia,max}}$  at preferred SF ( $p = 0.05$ ), but not for the other SFs.

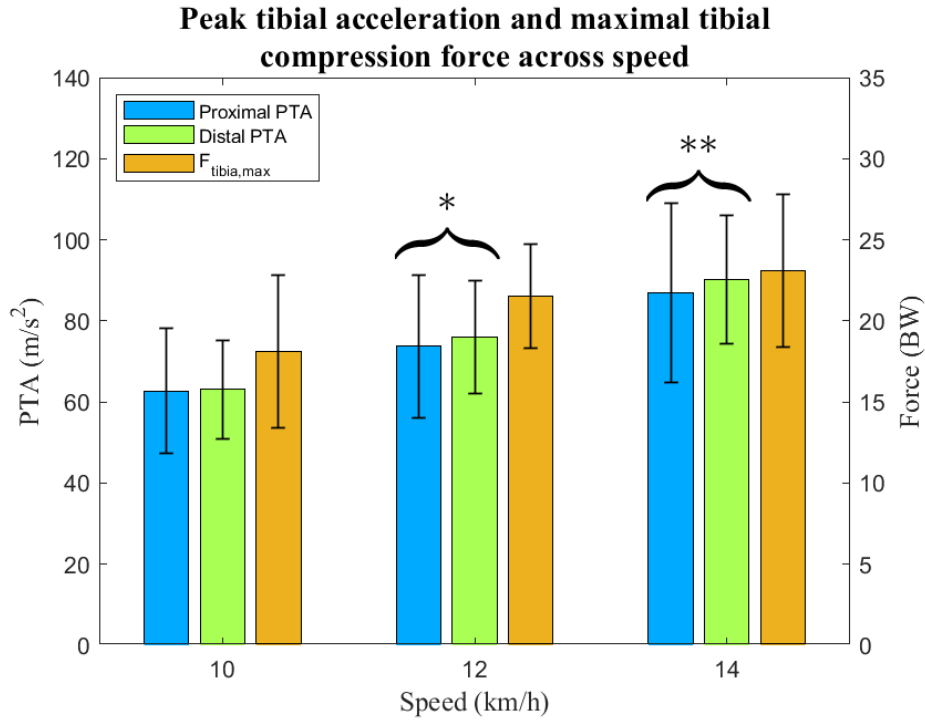


**Fig. 6** Mean PTA  $\pm$  SD for proximal and distal accelerations and maximal tibial compression force ( $F_{tibia,max}$ ) during running at 10, 12 and 14 km/h at preferred SF (see also table 3 in Appendix-II and figures 11-16 in Appendix-IV). Significant difference between proximal PTA and distal PTA are annotated. An \* indicates significance at 0.05 level (2-tailed), \*\* indicates significance at 0.01 level (2-tailed).

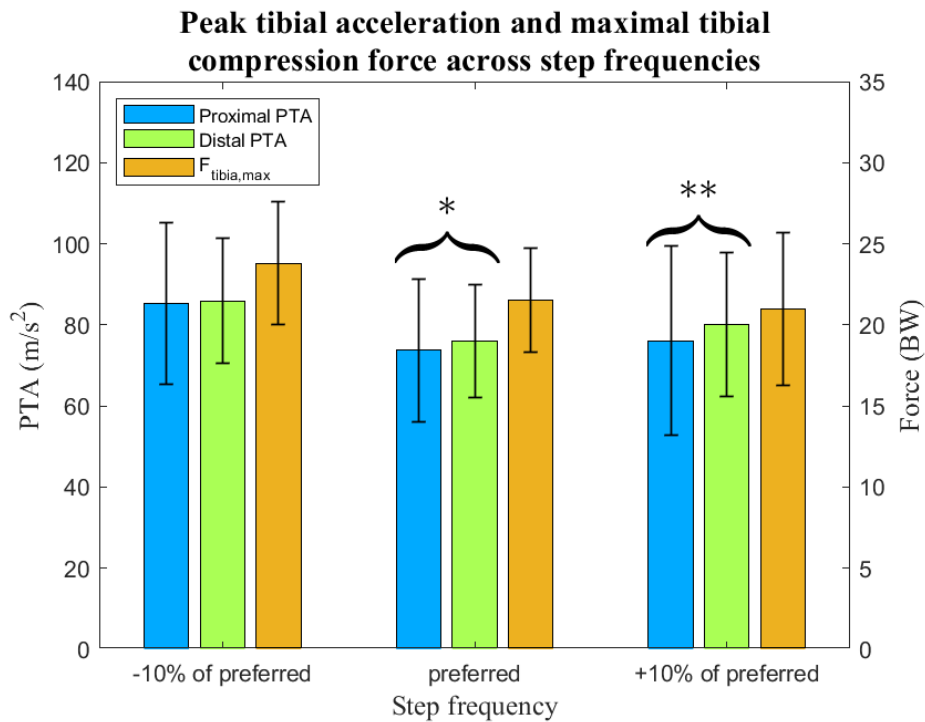


**Fig. 7** Mean PTA  $\pm$  SD for proximal and distal accelerations and maximal tibial compression force ( $F_{tibia,max}$ ) during running at preferred SF, ten percent below preferred SF and ten percent above preferred SF at 12 km/h (see also table 3 in Appendix-II and figures 17-22 in Appendix-V). Significant difference between proximal PTA and distal PTA are annotated. An \* indicates significance at 0.05 level (2-tailed), \*\* indicates significance at 0.01 level (2-tailed).

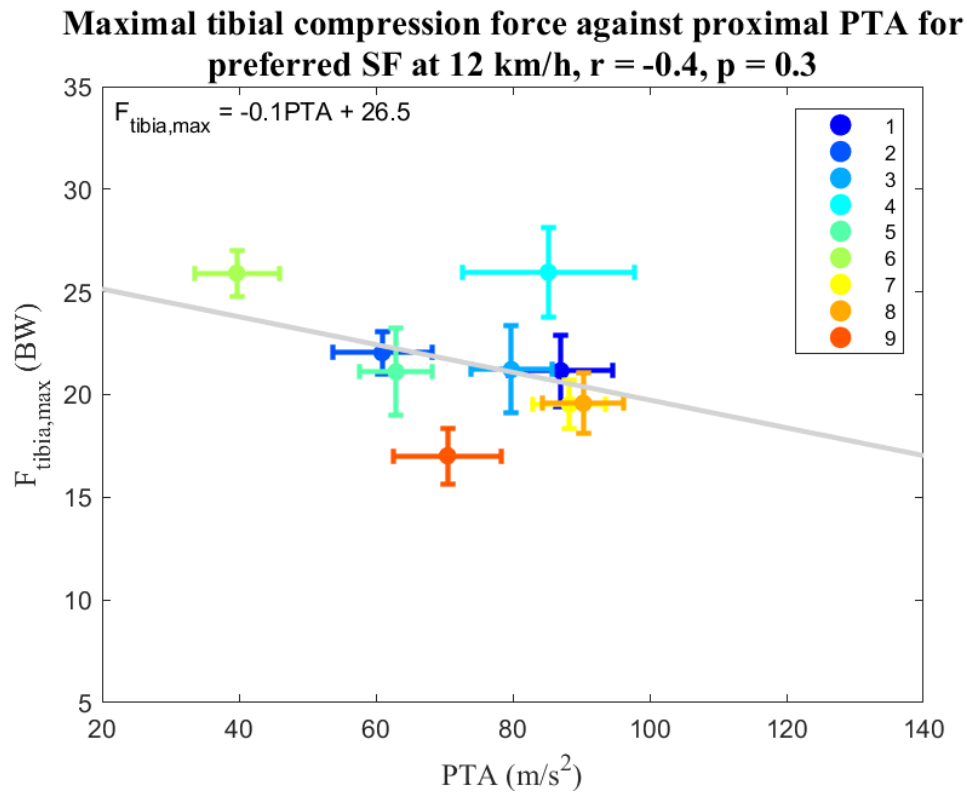


**Fig. 8** Scatter plot of mean  $\pm$  SD maximal tibial compression force ( $F_{tibia,max}$ ) against mean  $\pm$  SD proximal PTA for 12 km/h at preferred SF for each runner.

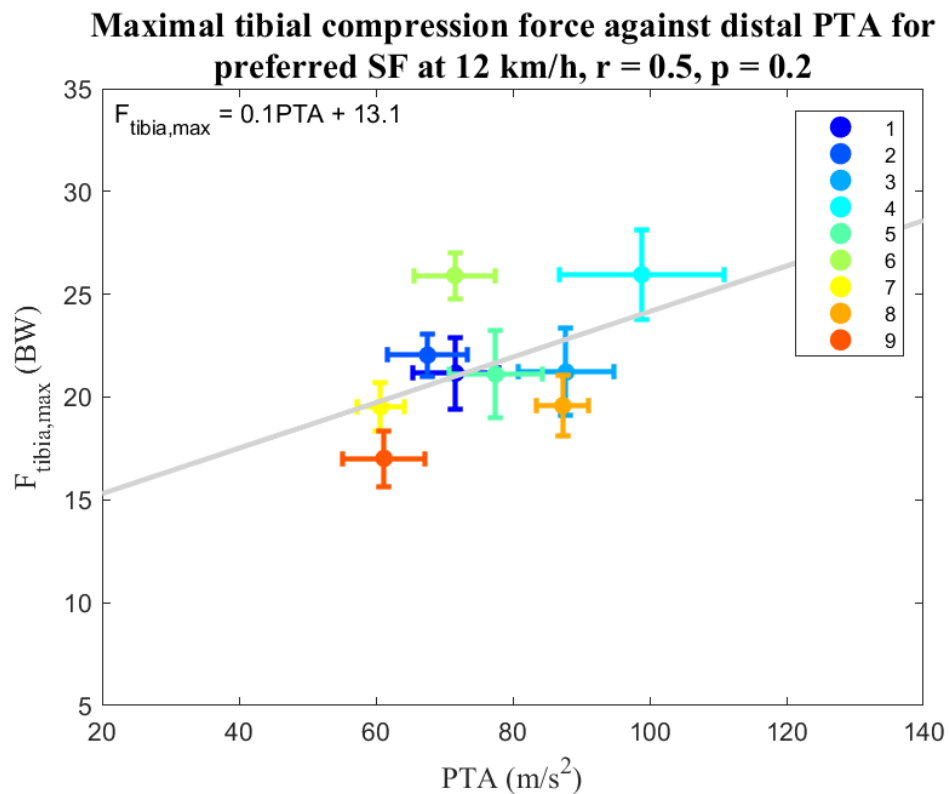


**Fig. 9** Scatter plot of mean  $\pm$  SD maximal tibial compression force ( $F_{tibia,max}$ ) against mean  $\pm$  SD distal PTA for 12 km/h at preferred SF for each runner.

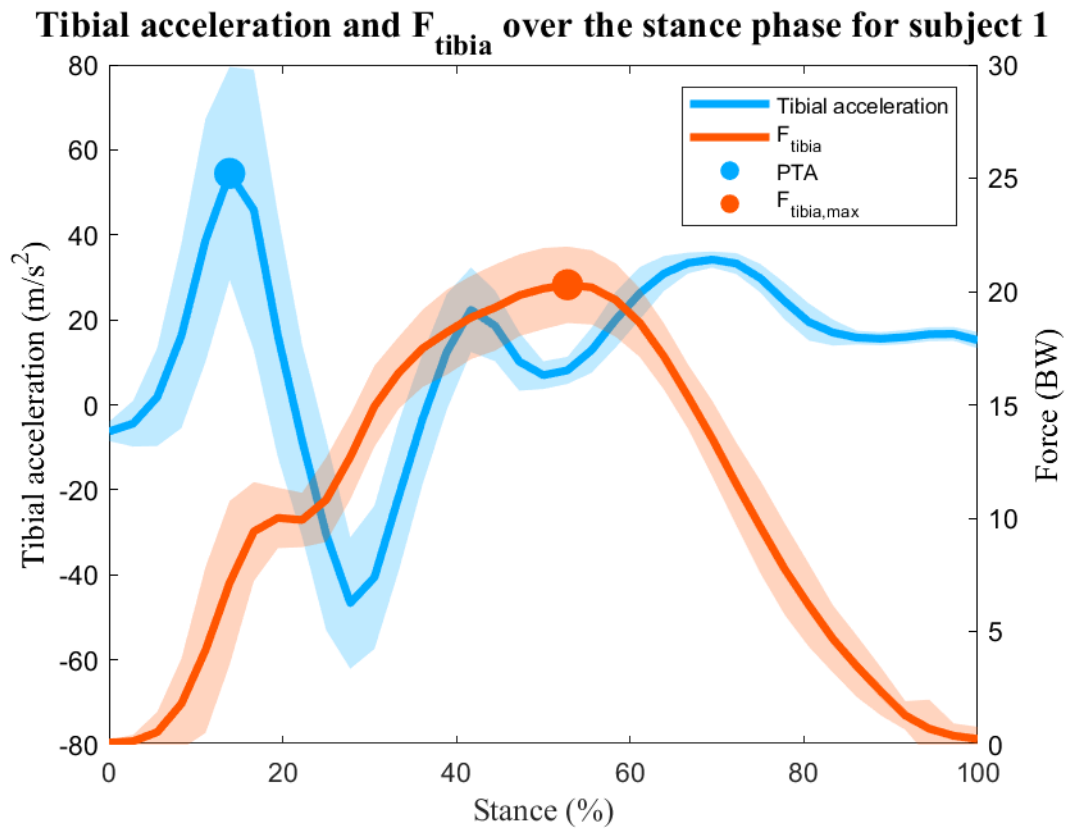


**Fig. 10** Mean  $\pm$  SD of 40 gait cycles of proximal tibial acceleration and  $F_{\text{tibia}}$  for runner 1 over the stance phase at 12 km/h, preferred SF. PTA and  $F_{\text{tibia,max}}$  are annotated.

**Table 1**

Pearson's  $r$  between PTA and maximal tibial compression force for every runner and all runners together for every speed at preferred SF.

| Runner         | Speed    |        |          |        |          |        |
|----------------|----------|--------|----------|--------|----------|--------|
|                | 10       |        | 12       |        | 14       |        |
|                | Proximal | Distal | Proximal | Distal | Proximal | Distal |
| <b>1</b>       | -0.1     | 0.3    | 0.3      | 0.4**  | 0.4**    | 0.5**  |
| <b>2</b>       | -0.2     | -0.2   | 0.2      | 0.2    | 0.0      | 0.1    |
| <b>3</b>       | -0.3*    | -0.2   | 0.0      | 0.1    | 0.0      | 0.1    |
| <b>4</b>       | -0.2     | -0.1   | -0.2     | -0.4*  | 0.2      | 0.0    |
| <b>5</b>       | 0.4**    | 0.5**  | 0.4*     | 0.2    | 0.2      | 0.2    |
| <b>6</b>       | 0.4*     | -0.3   | 0.1      | 0.0    | -0.3*    | -0.3   |
| <b>7</b>       | -0.1     | -0.1   | -0.3*    | -0.4*  | -0.1     | 0.3    |
| <b>8</b>       | -0.4**   | -0.3   | 0.1      | 0.0    | -0.4*    | -0.3*  |
| <b>9</b>       | -0.4**   | -0.5** | -0.2     | -0.2   | 0.5**    | 0.5**  |
| <b>Overall</b> | -0.9**   | -0.4   | -0.4     | 0.5    | -0.5     | -0.1   |

Correlation between PTA and maximal tibial compression force ( $F_{tibia,max}$ ) at 10, 12 and 14 km/h at preferred SF. Overall correlations were calculated by taking the mean of every runner, which is different than GEE (see figure 8 and 9 and Appendix-IV). An \* indicates significance at 0.05 level (2-tailed), \*\* indicates significance at 0.01 level (2-tailed).

**Table 2**

Pearson's  $r$  between PTA and maximal tibial compression force for every runner and all runners together for every SF at 12 km/h.

| Runner         | Step frequency |        |           |        |          |        |
|----------------|----------------|--------|-----------|--------|----------|--------|
|                | -10%           |        | Preferred |        | +10%     |        |
|                | Proximal       | Distal | Proximal  | Distal | Proximal | Distal |
| <b>1</b>       | 0.2            | 0.3    | 0.3       | 0.4**  | 0.2      | 0.2    |
| <b>2</b>       | 0.1            | 0.1    | 0.2       | 0.2    | -0.1     | -0.2   |
| <b>3</b>       | -0.3           | -0.2   | 0.0       | 0.1    | -0.1     | -0.1   |
| <b>4</b>       | -0.6**         | -0.6** | -0.2      | -0.4*  | -0.3*    | -0.5** |
| <b>5</b>       | 0.1            | 0.0    | 0.4*      | 0.2    | -0.1     | -0.1   |
| <b>6</b>       | -0.3           | -0.2   | 0.1       | 0.0    | 0.1      | 0.1    |
| <b>7</b>       | -0.4*          | -0.4*  | -0.3*     | -0.4*  | -0.1     | -0.1   |
| <b>8</b>       | 0.2            | 0.3    | 0.1       | 0.0    | -0.3     | 0.0    |
| <b>9</b>       | 0.4*           | 0.4*   | -0.2      | -0.2   | -0.2     | -0.3*  |
| <b>Overall</b> | -0.4           | 0.3    | -0.4      | 0.5    | -0.5     | -0.2   |

Correlation between PTA and maximal tibial compression force ( $F_{tibia,max}$ ) at preferred SF, ten percent below preferred SF and ten percent above preferred SF for 12 km/h. Overall correlations were calculated by taking the mean of every runner, which is different than GEE (see figure 8 and 9 and Appendix-V). An \* indicates significance at 0.05 level (2-tailed), \*\* indicates significance at 0.01 level (2-tailed).

## Discussion

This study aimed to assess the agreement between PTA and tibial bone loading (assessed by  $F_{\text{tibia,max}}$ ) to gain insight in the validity of PTA as an indicator of tibial bone loading. In support of the hypothesis, it was found that PTA positively correlated with speed, regardless of accelerometer location. PTA also tended to negatively correlate with SF, as hypothesized, but this was not the case for all runners. The strength of response of PTA to changes in SF was not consistent between proximal and distal accelerometers. Distal PTA tended to be higher than proximal PTA, but this was not significant at all conditions. In support of the hypothesis, tibial bone loading tended to increase for increases in speed. However, the strength of this relationship differed strongly per runner. Responses of tibial bone loading to changes in SF differed per runner in both direction and strength. Correlations between PTA and tibial bone loading were not consistent across conditions.

### PTA and $F_{\text{tibia,max}}$ at 12 km/h, preferred SF

At 12 km/h, preferred SF, PTA values (both distal and proximal) fell in the range of 40 to 100  $\text{m/s}^2$  (see figure 8 and 9), which is similar to PTA values found at earlier studies for comparable conditions [23,28,64,65]. Tibial bone loading, expressed as  $F_{\text{tibia,max}}$ , fell in the range of 15 to 25 BW (see figures 6-9, Appendix-IV and Appendix-V). This is higher in comparison with earlier studies, who reported 5-10 BW values for tibial bone loading at similar conditions [19,66]. This is mainly caused by a high internal force (muscle force), which is the result of a high ankle moment. Ankle moments in this study were found to be equal to approximately 8 Nm/kg. However, ankle moments for these kind of speeds tend to fall more into the 3-4 Nm/kg range [67–69]. An explanation for this lies in the spatial alignment of the force plate data with the musculoskeletal model. In practice, it was hard to align the two because the musculoskeletal model and the inverse kinematics data, which were calculated with OpenSense, do not have a clearly defined, fixed coordinate system. The alignment of the force plate and the musculoskeletal model was now based on the assumption that during IC, COM of the calcaneus and COP are equal. However, COP at IC is equal to the point which is in contact with the ground, which is not necessarily equal to COM of the calcaneus. Therefore, a small offset existed between actual COP and COP which was based on COM of the calcaneus, which could have influenced the magnitude of the ankle moments. Choosing COM of the talus, instead of the COM of the calcaneus, might have provided different solutions, as it could possibly be closer to the actual contact point of the foot during impact, and thus the COP. However, it is important here to realize that still some offset would exist between COM and COP.

Furthermore, most runners displayed a higher distal PTA than proximal PTA (see also table 3 in Appendix-II). This was also observed on a group level (where distal PTA was 3% higher than proximal PTA) and is in accordance with previous research [23]. An explanation for this is the angular motion of the tibia during running. The proximal sensor is located further away from the ankle. As a result, the centripetal acceleration at the proximal site is higher, which leads to a lower axial acceleration, and so proximally measured PTA is generally lower than distal PTA. Some runners had a lower distal PTA, which can be explained by external factors, such as soft tissue artefacts. The skin underneath the distal sensor then acts as a damper, which leads to a lower distal PTA.

### PTA and tibial bone loading across different speeds

The majority of the runners demonstrated higher tibial bone loading and higher PTA at a higher speed, regardless of accelerometer location (see also left side of table 4 in Appendix-

III). This is in accordance with existing literature [28,31,38,70]. Increases in speed could lead to a change in foot strike patterns and subsequently in a change in tibial bone loading and PTA [71]. When running at a higher speed, runners tend to land 'higher' on the foot (more on mid-foot/forefoot) [72,73]. This was also observed in the videos made of the feet and lower legs. Such a landing is associated with higher muscle activity and would thus lead to a higher loading on the tibia [38,74–77]. Higher speeds also lead to heavier landings, which explained the increase in PTA for higher speeds [42,65]. One runner demonstrated a decrease in tibial bone loading for higher speeds. This runner could possibly have a preferred way of running at certain speeds, which could, for example, be explained by experience, which resulted in lower loading on the tibia. This highlights the importance of understanding the response of each individual athlete.

### **PTA and tibial bone loading across different SFs**

Runners demonstrated different PTA responses to changes in SF and were not all significant (see also right side of table 4 in Appendix-III). Some runners showed a lower PTA for a higher SF, which is in accordance with existing literature [78,79]. Running at a higher SF leads to a lower step width, which is associated with a greater knee flexion angle at impact [31]. As a result, lower impact forces are experienced by the body, which would lead to lower PTA [78]. One runner demonstrated a decrease in PTA for running at a lower SF. This could also be explained by having a preferred way of running at certain SFs, which could lead to higher PTA at higher SFs.

Some runners showed no significant change in PTA for changes in SF. This could be because there was not enough change in SF [32,34]. Runners found it difficult to run at other SFs than their own SF, especially running at a lower SF was considered hard. Some runners were not able to run at ten percent from their preferred SF and their measured SF was closer to a five percent change from their preferred SF than to a ten percent change (see also table 5 in Appendix-VI). Earlier research has suggested that a minimum change in SF of ten percent is required to observe an effect in PTA [34]. This could explain the lack of response in PTA to changes in SF. Alternatively, the inexperience of runners for running at other SFs could have led them to run in such a way at other SFs that the effect of SF on PTA was reduced.

Tibial bone loading tended to be negatively associated with SF, which is in accordance with existing literature [66]. When running at a higher SF, the heel will horizontally be closer to COM at IC, which leads to a decrease in the knee flexion angle. This leads to a lower ankle moment (which was in this study used to calculate the contribution of muscle forces), and thus a lower loading on the tibia [66,80]. One runner had higher tibial bone loading at higher SFs. This could be explained by a change in foot strike pattern as a response to running at another SF. When running at a higher SF, runners tend to switch to a forefoot strike pattern [73]. This was also observed in the videos, which were made from the feet and lower legs. As a result, the plantar flexion angle increases, such that COP is located anterior to the ankle. To control then the descent of the heel during the stance phase, the gastrocnemius and soleus need to generate a greater moment, which thus results in a higher loading on the tibia [41,61,79]. Similar to PTA, some runners reported no significant change in tibial bone loading to changes in SF. This could be explained by an insufficient change in SF to observe an effect, as some runners found it hard to run at different SFs. Alternatively, the inexperience of the runner to run at different SFs could have impacted their way of running in such a way that a possible effect on tibial bone loading was also affected.

Distally measured PTA tended to respond similarly to changes in SF as proximal PTA. This is explained by the fact that proximal PTA and distal PTA essentially measure the same,

but at a different location. The proximal sensor is located further away from the ankle, which results in a higher centripetal acceleration at the proximal site and in turn a lower axial acceleration. As a result, proximally measured PTA will generally be lower than distal PTA [81]. For some runners, the response of distal and proximal PTA to a change in SF was not consistent. Perhaps runners changed their way of running at unfamiliar SFs in such a way that distal and proximal PTA responded differently.

### **Agreement between PTA and $F_{\text{tibia,max}}$**

Correlations between  $F_{\text{tibia,max}}$  and proximal PTA varied a lot across conditions and across runners and tended to be weak (see also table 1 and 2, figure 8 and 9, and Appendix-IV and Appendix-V). This is in accordance with earlier research which compared GRF-based metrics (which are often highly correlated with PTA) with tibial bone loading [19,22,28,36,37]. An explanation for this lies in the relative high contribution of muscle forces to the total loading on the tibia bone (about 75% of total force, 5-6 BW, see also figure 1) [19]. PTA only measures the impact force, but this force only accounts for a small part of the total force (see also figure 1). It can also be seen in figure 10 that the peak in the acceleration signal occurs at the beginning of the stance phase, while the peak in the  $F_{\text{tibia}}$  occurs much later. Therefore, using PTA as an indicator of tibial bone loading may provide limited understanding of how loading on the bone changes across different speeds and SFs and thus may provide limited indication of tibial stress fracture risk.

A strong, negative correlation was found at one condition (10 km/h, preferred SF, see Appendix-IV) on a group level. However, when looking at every runner separately, no significant correlations of such strength are found for any of the runners. While the correlation on the group level may have statistical significance, it seems unlikely that this correlation also has practical significance. For instance, a negative correlation would indicate that when PTA increases (or essentially, the impact force increases), the total force acting on the tibia would decrease.

### **Limitations**

A limitation of this study is the validity of the used tibial bone loading metric. The found values for the loading on the tibia in this study are considerably higher than values found in earlier studies [6,19,66]. This is mainly explained by the assumptions which needed to be made in order to calculate the ankle kinetics, which were used to calculate the internal force, similar to [19]. In this study, a musculoskeletal model of Rajagopal was used. This model models the ankle joint as a revolute joint and has been developed to compute kinematics and kinetics for running trials [50,52]. It is important here to realize, as also highlighted in the introduction, that biomechanical modelling needs to make assumptions about certain parameters to come to a solution, which could impact the results [17]. Besides, the model in this study was linearly scaled based on the height of each runner, which could have led to inaccuracies in the resultant model. Linear scaling does not account for inter-individual anatomical variations and can lead to inaccurate joint moment arms, which might provide an explanation for the high ankle moments in this study [82,83]. It was not possible here to scale the model non-linearly, because IMUs were used to construct the model. Future research could therefore focus on improving musculoskeletal models obtained from IMUs.

OpenSense, an extension of OpenSim, was used to calculate the kinematics from IMU data, based on a weighted least squares (see also Appendix-I). The use of IMUs to calculate kinematics has increased over the years, but methods to calculate these kinematics from IMUs differ and are application dependent [84]. The OpenSense method has mainly been applied in

walking and its application in studies is limited [85,86]. It is therefore unclear whether the algorithm is also stable for the conditions used in this study, which could have impacted the moment arms and thus the found ankle moments. Kinematics calculated in this study seemed to fall within the normal joint angle range for these kinds of conditions. However, a large range of motion (ROM) for the hip adduction angle was observed. Hip adduction ROM for running tends to be 15-20 deg, but in this study it was approximately 30 deg [87]. This could possibly have impacted the results.

Besides, some assumptions needed to be made to align the force plate data with the musculoskeletal model, because the kinematics from OpenSim are not expressed in a clearly defined, fixed coordinate system. It was now assumed that during IC, COM of the calcaneus and COP are equal. However, COP at IC is equal to the point which is in contact with the ground, which is not necessarily equal to COM of the calcaneus (or talus). The small offset (estimated at about 3-5 cm) which existed between COP and COM of the calcaneus could have impacted the joint moment arms and thus the joint moments [88,89].

Furthermore, FM was set to zero in this study. FM has been neglected before in research, mainly because it was very small [58]. However, these applications were mainly used for walking trials, instead of running. It has been found that FM increases with gait speed, but this was focused on walking [90]. In comparison, FM in walking has been found to be equal to 0.002-0.004 %BW\*height, while in running FM values have been reported of 0.005-0.009 %BW\*height [57,91]. Therefore, FM in this study was also set to zero for the inverse dynamics calculations due to its limited contribution. However, this could have had an impact on the obtained ankle moments in this study and thus on the calculated tibial bone loading metric. Nevertheless, this impact is expected to be small, as FM has such a small value. All in all, further research is needed to establish a method to align kinematics data obtained from inertial motion capture systems with force plate data to calculate kinetics. An indirect solution for this is estimating kinetic data from IMUs. This has already been proposed by research, in which kinetics from IMU data are estimated using machine learning or optimal control [92-94]. However, more research is needed in how force plate data and IMU data can be combined to form conclusions about human movement, specifically in the alignment of the force data and the kinematics data.

In this study, PTA was compared with a tibial bone loading metric which was also used by [19]. This metric accounted for the compressive force acting on the tibia and assumes that the ankle force is indicative of tibial compression force. It has been found to produce similar values to tibial bone loading with other studies, including cadaver studies [6,16]. This metric assumes that the force acting on the tibia can be estimated by summing an external force and an internal force. The internal force, muscle force, was estimated in this study by dividing the ankle moment by the Achilles tendon moment arm (see figure 5). Comparison of this method with static optimization has found similar results [62]. This method does not account for muscle co-activation, which could lead to an underestimation of the muscle force. However, previous research indicates that this does not influence the peak muscle forces, as it only seems to occur in the early stance phase [62]. Furthermore, the used tibial force metric has been used before in research, but not extensively. It remains therefore the question whether the used method gives valid results for the force acting on the tibia. Besides, this method only considers the compressive force acting on the tibia, but other forces, such as bending, shear or torsional forces may also be important in the onset of stress fractures. It is unclear how PTA correlates with those forces, so future research could focus on the importance of other forces during the onset of tibia stress fractures, and if and how these forces correlate with PTA.

This study also only looked at maximal tibial compression force, i.e., the magnitude of the load. The magnitude of the load can be used to say something about the cyclic fatigue, the forces which are acting on the bone. Nevertheless, looking at only the maximal force neglects the influence of cumulative loading on the bone over time [95]. Therefore, future studies could focus on also taking cumulative loading in account, for example by taking the time integral of the force, similar to [19].

In this study, limited effects were reported for changing SF on tibial bone loading and PTA. Most runners reported that they found it difficult to run at other SFs, especially at the lower SFs. This could be explained by a lack of experience of the runners for running at another SF. As a result, relative change of actual SF was more equal to five percent for some runners, instead of the intended ten percent, as can be viewed in Appendix-VI. This could have impacted the results and might provide an explanation for the limited effect of changing SF on PTA and tibial bone loading. Besides, runners were not trained in running at unfamiliar SFs, which could have impacted their way of running and subsequently PTA and tibial bone loading. Therefore, future studies should take a longer adjustment period into account when changing SF or should first train runners in running at lower SFs.



### **Conclusion**

This research assessed the agreement between PTA and maximal tibial compression force in runners across different conditions. Findings of the present study demonstrate that the use of PTA as a surrogate for the forces acting on the tibia during running might not be appropriate. Correlations between runners differed and were mostly absent or weak. Besides, correlations were found to be both positive and negative, which indicates that conclusions about PTA as an indicator of tibial bone loading should be taken with caution. However, it is important here to question the validity of the used tibial bone loading metric in this study when interpreting the results. Found values for tibial bone loading differ strongly from previous research, which shows the need for a valid way to calculate tibial bone loading from IMUs. Besides, attention should be given in future studies in how the loading on the tibia is calculated and should account for the effects of torsional and shear forces. In conclusion, this research has added to the existing literature which questions the use of PTA as an indicator of tibial bone loading.



### References

- [1] Van Gent RN, Siem D, Van Middelkoop M, Van Os AG, Bierma-Zeinstra SMA, Koes BW. Incidence and determinants of lower extremity running injuries in long distance runners: A systematic review. *Br J Sports Med* 2007;41:469–80. doi:10.1136/bjism.2006.033548.
- [2] Taunton JE, Ryan MB, Clement DB, McKenzie DC, Lloyd-Smith DR, Zumbo BD. A prospective study of running injuries: The Vancouver Sun Run “In Training” clinics. *Br J Sports Med* 2003;37:239–44. doi:10.1136/bjism.37.3.239.
- [3] Bennell KL, Malcolm SA, Thomas SA, Wark JD, Brukner PD. The incidence and distribution of stress fractures in competitive track and field athletes: A twelve-month prospective study. *Am J Sports Med* 1996;24:211–7. doi:10.1177/036354659602400217.
- [4] Brukner P, Khan KM, Crossley KM. Stress fractures: A review of 180 cases. *Clin J Sport Med* 1996;6:85–9.
- [5] Lopes AD, Hespanhol LC, Yeung SS, Costa LOP. What are the Main Running-Related Musculoskeletal Injuries? *Sport Med* 2012;42:891–905. doi:10.1007/bf03262301.
- [6] Sasimontongkul S, Bay BK, Pavol MJ. Bone contact forces on the distal tibia during the stance phase of running. *J Biomech* 2007;40:3503–9. doi:10.1016/j.jbiomech.2007.05.024.
- [7] Scott SH, Winter DA. Internal forces at chronic running injury sites. *Med Sci Sports Exerc* 1990;22:357–69. doi:10.1249/00005768-199006000-00013.
- [8] Burdett RG. Forces predicted at the ankle during running. *Med Sci Sport Exerc* 1982;14:308–16. doi:10.1249/00005768-198204000-00010.
- [9] Meardon SA, Willson JD, Gries SR, Kernozek TW, Derrick TR. Bone stress in runners with tibial stress fracture. *Clin Biomech* 2015;30:895–902. doi:10.1016/j.clinbiomech.2015.07.012.
- [10] Warden SJ, Burr DB, Brukner PD. Stress fractures: Pathophysiology, epidemiology, and risk factors. *Curr Osteoporos Rep* 2006;4:103–9. doi:10.1007/s11914-996-0029-y.
- [11] Al Nazer R, Lanovaz J, Kawalilak C, Johnston JD, Kontulainen S. Direct in vivo strain measurements in human bone—A systematic literature review. *J Biomech* 2012;45:27–40. doi:10.1016/j.jbiomech.2011.08.004.
- [12] Parashar SK, Sharma JK. A review on application of finite element modelling in bone biomechanics. *Perspect Sci* 2016;8:696–8. doi:10.1016/j.pisc.2016.06.062.
- [13] Ruchirabha T, Puttapitukporn T, Sasimontongkul S. Study of stress distribution in the tibia during stance phase running using the finite element method. *Agric Nat Resour* 2014;48:729–39.
- [14] Meardon SA, Derrick TR. Effect of step width manipulation on tibial stress during running. *J Biomech* 2014;47:2738–44. doi:10.1016/j.jbiomech.2014.04.047.
- [15] Edwards WB, Taylor D, Rudolphi TJ, Gillette JC, Derrick TR. Effects of Stride Length and Running Mileage on a Probabilistic Stress Fracture Model. 2009. doi:10.1249/MSS.0b013e3181a984c4.
- [16] Sharkey NA, Hamel AJ. A dynamic cadaver model of the stance phase of gait: Performance characteristics and kinetic validation. *Clin Biomech* 1998;13:420–33. doi:10.1016/S0268-0033(98)00003-5.
- [17] Sawers AB, Hahn ME. The Potential for Error With Use of Inverse Dynamic

- Calculations in Gait Analysis of Individuals With Lower Limb Loss: A Review of Model Selection and Assumptions. *JPO J Prosthetics Orthot* 2010;22:56–61. doi:10.1097/JPO.0b013e3181cba08b.
- [18] Zadpoor AA, Nikooyan AA. The relationship between lower-extremity stress fractures and the ground reaction force: A systematic review. *Clin Biomech* 2011;26:23–8. doi:10.1016/j.clinbiomech.2010.08.005.
- [19] Matijevich ES, Branscombe LM, Scott LR, Zelik KE. Ground reaction force metrics are not strongly correlated with tibial bone load when running across speeds and slopes: Implications for science, sport and wearable tech. *PLoS One* 2019;14:e0210000. doi:10.1371/journal.pone.0210000.
- [20] Loundagin LL, Schmidt TA, Brent Edwards W. Mechanical Fatigue of Bovine Cortical Bone Using Ground Reaction Force Waveforms in Running. *J Biomech Eng* 2018;140:0310031. doi:10.1115/1.4038288.
- [21] Engsborg JR, Hanley DA. Bone mass, external loads, and stress fracture in female runners. *J Appl Biomech* 1991. doi:10.1123/ijsb.7.3.293.
- [22] Matijevich ES, Scott LR, Volgyesi P, Derry KH, Zelik KE. Combining wearable sensor signals, machine learning and biomechanics to estimate tibial bone force and damage during running. *Hum Mov Sci* 2020;74:102690. doi:10.1016/j.humov.2020.102690.
- [23] Lucas-Cuevas AG, Encarnación-Martínez A, Camacho-García A, Llana-Belloch S, Pérez-Soriano P. The location of the tibial accelerometer does influence impact acceleration parameters during running. *J Sports Sci* 2017;35:1734–8. doi:10.1080/02640414.2016.1235792.
- [24] Tirosch O, Orland G, Eliakim A, Nemet D, Steinberg N. Repeatability of tibial acceleration measurements made on children during walking and running. *J Sci Med Sport* 2019;22:91–5. doi:10.1016/j.jsams.2018.04.006.
- [25] Raper DP, Witchalls J, Philips EJ, Knight E, Drew MK, Waddington G. Use of a tibial accelerometer to measure ground reaction force in running: a reliability and validity comparison with force plates. *J Sci Med Sport* 2018;21:84–8. doi:10.1016/j.jsams.2017.06.010.
- [26] Sheerin K, Besier T, Reid D, Hume P. The reliability and variability of three-dimensional tibial acceleration during running. *ISBS-Conference Proc. Arch.*, 2016.
- [27] Sheerin KR, Besier TF, Reid D, Hume PA. The one-week and six-month reliability and variability of three-dimensional tibial acceleration in runners. *Sport Biomech* 2018;17:531–40. doi:10.1080/14763141.2017.1371214.
- [28] Van den Berghe P, Six J, Gerlo J, Leman M, De Clercq D. Validity and reliability of peak tibial accelerations as real-time measure of impact loading during over-ground rearfoot running at different speeds. *J Biomech* 2019;86:238–42. doi:10.1016/j.jbiomech.2019.01.039.
- [29] Norris M, Anderson R, Kenny IC. Method analysis of accelerometers and gyroscopes in running gait: A systematic review. *Proc Inst Mech Eng Part P J Sport Eng Technol* 2014;228:3–15. doi:10.1177/1754337113502472.
- [30] Reenalda J, Maartens E, Buurke JH, Gruber AH. Kinematics and shock attenuation during a prolonged run on the athletic track as measured with inertial magnetic measurement units. *Gait Posture* 2019;68:155–60. doi:10.1016/j.gaitpost.2018.11.020.
- [31] Sheerin KR, Reid D, Besier TF. The measurement of tibial acceleration in runners—A

- review of the factors that can affect tibial acceleration during running and evidence-based guidelines for its use. *Gait Posture* 2019;67:12–24. doi:10.1016/j.gaitpost.2018.09.017.
- [32] Clarke TE, Cooper LB, Hamill CL, Clark DE. The effect of varied stride rate upon shank deceleration in running. *J Sports Sci* 1985;3:41–9. doi:10.1080/02640418508729731.
- [33] Busa MA, Lim J, van Emmerik REA, Hamill J. Head and Tibial Acceleration as a Function of Stride Frequency and Visual Feedback during Running. *PLoS One* 2016;11:e0157297. doi:10.1371/journal.pone.0157297.
- [34] Schubert AG, Kempf J, Heiderscheit BC. Influence of Stride Frequency and Length on Running Mechanics: A Systematic Review. *Sports Health* 2014. doi:10.1177/1941738113508544.
- [35] Francis P, Whatman C, Sheerin K, Hume P, Johnson MI. The proportion of lower limb running injuries by gender, anatomical location and specific pathology: A systematic review. *J Sport Sci Med* 2019;18:21–31.
- [36] Hennig EM, Lafortune MA. Relationships between Ground Reaction Force and Tibial Bone Acceleration Parameters. *Int J Sport Biomech* 2016;7:303–9. doi:10.1123/ijsb.7.3.303.
- [37] Hennig EM, Milani TL, Lafortune MA. Use of Ground Reaction Force Parameters in Predicting Peak Tibial Accelerations in Running. *J Appl Biomech* 1993;9:306–14. doi:10.1123/jab.9.4.306.
- [38] Kyröläinen H, Avela J, Komi P V. Changes in muscle activity with increasing running speed. *J Sports Sci* 2005;23:1101–9. doi:10.1080/02640410400021575.
- [39] Chumanov ES, Wille CM, Michalski MP, Heiderscheit BC. Changes in muscle activation patterns when running step rate is increased. *Gait Posture* 2012;36:231–5. doi:10.1016/j.gaitpost.2012.02.023.
- [40] Lenhart RL, Thelen DG, Wille CM, Chumanov ES, Heiderscheit BC. Increasing running step rate reduces patellofemoral joint forces. *Med Sci Sports Exerc* 2014;46:557–64. doi:10.1249/MSS.0b013e3182a78c3a.
- [41] Kernozek TW. Effects of Foot Strike and Step Frequency on Achilles Tendon Stress During Running. *Artic J Appl Biomech* 2016. doi:10.1123/jab.2015-0183.
- [42] Ruder M, Jamison ST, Tenforde A, Mulloy F, Davis IS. Relationship of Foot Strike Pattern and Landing Impacts during a Marathon. *Med Sci Sports Exerc* 2019;51:2073–9. doi:10.1249/MSS.0000000000002032.
- [43] Xsens. MVN User Manual 2015. [https://www.xsens.com/hubfs/Downloads/usermanual/MVN\\_User\\_Manual.pdf](https://www.xsens.com/hubfs/Downloads/usermanual/MVN_User_Manual.pdf) (accessed December 7, 2021).
- [44] Gruber AH, Edwards WB, Hamill J, Derrick TR, Boyer KA. A comparison of the ground reaction force frequency content during rearfoot and non-rearfoot running patterns. *Gait Posture* 2017;56:54–9. doi:10.1016/j.gaitpost.2017.04.037.
- [45] Tenforde AS, Hayano T, Jamison ST, Outerleys J, Davis IS. Tibial Acceleration Measured from Wearable Sensors Is Associated with Loading Rates in Injured Runners. *PM&R* 2020;12:679–84. doi:10.1002/pmrj.12275.
- [46] Karatsidis A, Bellusci G, Schepers H, de Zee M, Andersen M, Veltink P. Estimation of Ground Reaction Forces and Moments During Gait Using Only Inertial Motion Capture. *Sensors* 2016;17:75. doi:10.3390/s17010075.

- [47] Preparing Force Data - OpenSim Documentation - Algemene site n.d. <https://simtk-confluence.stanford.edu:8443/display/OpenSim/Preparing+Force+Data> (accessed November 26, 2021).
- [48] Mai P, Willwacher S. Effects of low-pass filter combinations on lower extremity joint moments in distance running. *J Biomech* 2019;95:109311. doi:10.1016/j.jbiomech.2019.08.005.
- [49] Reenalda J, Zandbergen MA, Harbers JHD, Paquette MR, Milner CE. Detection of foot contact in treadmill running with inertial and optical measurement systems. *J Biomech* 2021;121:110419. doi:10.1016/j.jbiomech.2021.110419.
- [50] Rajagopal A, Dembia CL, DeMers MS, Delp DD, Hicks JL, Delp SL. Full-Body Musculoskeletal Model for Muscle-Driven Simulation of Human Gait. *IEEE Trans Biomed Eng* 2016;63:2068–79. doi:10.1109/TBME.2016.2586891.
- [51] Chen TLW, Wong DWC, Wang Y, Lin J, Zhang M. Foot arch deformation and plantar fascia loading during running with rearfoot strike and forefoot strike: A dynamic finite element analysis. *J Biomech* 2019;83:260–72. doi:10.1016/j.jbiomech.2018.12.007.
- [52] Yong JR, Silder A, Montgomery KL, Fredericson M, Delp SL. Acute changes in foot strike pattern and cadence affect running parameters associated with tibial stress fractures. *J Biomech* 2018;76:1–7. doi:10.1016/j.jbiomech.2018.05.017.
- [53] Delp SL, Anderson FC, Arnold AS, Loan P, Habib A, John CT, et al. OpenSim: Open-Source Software to Create and Analyze Dynamic Simulations of Movement. *IEEE Trans Biomed Eng* 2007;54. doi:10.1109/TBME.2007.901024.
- [54] Seth A, Hicks JL, Uchida TK, Habib A, Dembia CL, Dunne JJ, et al. OpenSim: Simulating musculoskeletal dynamics and neuromuscular control to study human and animal movement. *PLoS Comput Biol* 2018;14. doi:10.1371/journal.pcbi.1006223.
- [55] Willwacher S, Goetze I, Fischer KM, Brüggemann G-P. The free moment in running and its relation to joint loading and injury risk. *Footwear Sci* 2016;8:1–11. doi:10.1080/19424280.2015.1119890.
- [56] Willwacher S, Fischer K, Goetze I, Hamill J, Rohr E, Brüggemann GP. Free moment patterns, transversal plane joint loading and injury risk in running. *Footwear Sci* 2015;7:S124–6. doi:10.1080/19424280.2015.1038644.
- [57] Milner CE, Davis IS, Hamill J. Free moment as a predictor of tibial stress fracture in distance runners. *J Biomech* 2006;39:2819–25. doi:10.1016/j.jbiomech.2005.09.022.
- [58] Maeda T, Ishizuka T, Yamaji S, Ohgi Y. A Force Platform Free Gait Analysis †. *Proceedings* 2018;2:207. doi:10.3390/proceedings2060207.
- [59] Farris DJ, Sawicki GS. Human medial gastrocnemius force-velocity behavior shifts with locomotion speed and gait. *Proc Natl Acad Sci U S A* 2012;109:977–82. doi:10.1073/pnas.1107972109.
- [60] McCullough MBA, Ringleb SI, Arai K, Kitaoka HB, Kaufman KR. Moment arms of the ankle throughout the range of motion in three planes. *Foot Ankle Int* 2011;32:300–6. doi:10.3113/FAI.2011.0300.
- [61] Almonroeder T, Willson JD, Kernozek TW. The Effect of Foot Strike Pattern on Achilles Tendon Load During Running. *Ann Biomed Eng* 2013. doi:10.1007/s10439-013-0819-1.
- [62] Kernozek T, Gheidi N, Ragan R. Comparison of estimates of Achilles tendon loading from inverse dynamics and inverse dynamics-based static optimisation during running. *J Sports Sci* 2017;35:2073–9. doi:10.1080/02640414.2016.1255769.

- [63] Hopkins AG, Marshall SW, Batterham AM, Hanin J. Progressive Statistics for Studies in Sports Medicine and Exercise Science. *Med Sci Sport Exerc* 2009;41:3–12. doi:10.1249/MSS.0b013e31818cb278.
- [64] Mitschke C, Kiesewetter P, Milani T. The Effect of the Accelerometer Operating Range on Biomechanical Parameters: Stride Length, Velocity, and Peak Tibial Acceleration during Running. *Sensors* 2018;18:130. doi:10.3390/s18010130.
- [65] Brayne L, Barnes A, Heller B, Wheat J. Using a wireless inertial sensor to measure tibial shock during running: agreement with a skin mounted sensor. 2015.
- [66] Bowersock CD, Willy RW, DeVita P, Willson JD. Independent effects of step length and foot strike pattern on tibiofemoral joint forces during running. *J Sports Sci* 2017;35:2005–13. doi:10.1080/02640414.2016.1249904.
- [67] Petersen J, Nielsen RO, Rasmussen S, Sørensen H. Comparisons of increases in knee and ankle joint moments following an increase in running speed from 8 to 12 to 16 km·h<sup>-1</sup>. *Clin Biomech* 2014;29:959–64. doi:10.1016/j.clinbiomech.2014.09.003.
- [68] Lai AKM, Lichtwark GA, Schache AG, Pandy MG. Differences in in vivo muscle fascicle and tendinous tissue behavior between the ankle plantarflexors during running. *Scand J Med Sci Sports* 2018;28:1828–36. doi:10.1111/sms.13089.
- [69] de David AC, Carpes FP, Stefanyshyn D. Effects of changing speed on knee and ankle joint load during walking and running. *J Sports Sci* 2015;33:391–7. doi:10.1080/02640414.2014.946074.
- [70] Boey H, Aeles J, Schütte K, Vanwanseele B. Sports Biomechanics The effect of three surface conditions, speed and running experience on vertical acceleration of the tibia during running. *Taylor Fr* 2016;16:166–76. doi:10.1080/14763141.2016.1212918.
- [71] Sheerin KR, Besier TF, Reid D. The influence of running velocity on resultant tibial acceleration in runners. *Sport Biomech* 2018:1–11. doi:10.1080/14763141.2018.1546890.
- [72] Breine B, Malcolm P, Galle S, Fiers P, Frederick EC, De Clercq D. Running speed-induced changes in foot contact pattern influence impact loading rate. *Eur J Sport Sci* 2019;19:774–83. doi:10.1080/17461391.2018.1541256.
- [73] Allen DJ, Heisler H, Mooney J, Kring R. The effect of step rate manipulation on foot strike pattern of long distance runners. *Int J Sports Phys Ther* 2016;11:54–63.
- [74] Yong JR, Dembia CL, Silder A, Jackson RW, Fredericson M, Delp SL. Foot strike pattern during running alters muscle-tendon dynamics of the gastrocnemius and the soleus. *Sci Rep* 2020;10. doi:10.1038/s41598-020-62464-3.
- [75] Almonroeder T, Willson JD, Kernozek TW. The Effect of Foot Strike Pattern on Achilles Tendon Load During Running. Springer 2013. doi:10.1007/s10439-013-0819-1.
- [76] Kuhman D, Melcher D, Paquette MR. Ankle and knee kinetics between strike patterns at common training speeds in competitive male runners. *Taylor Fr* 2015;16:433–40. doi:10.1080/17461391.2015.1086818.
- [77] Jeon HM, Choi EB, Heo JH, Eom GM. Ankle joint moments in different foot strike methods during stair descent. *J Mech Med Biol* 2019;19. doi:10.1142/S0219519419400311.
- [78] Hobara H, Sakaguchi M, Nakazawa K. Step Frequency and Lower Extremity Loading During Running Sport. *Artic Int J Sport Med* 2012;33:310–3. doi:10.1055/s-0031-1291232.

- [79] Lyght M, Nockerts M, Kernozek TW, Ragan R. Effects of foot strike and step frequency on Achilles tendon stress during running. *J Appl Biomech* 2016;32:365–72. doi:10.1123/jab.2015-0183.
- [80] Thompson MA, Gutmann A, Seegmiller J, McGowan CP. The effect of stride length on the dynamics of barefoot and shod running. *J Biomech* 2014;47:2745–50. doi:10.1016/j.jbiomech.2014.04.043.
- [81] Lafortune M, and EH-M and science in sports, 1991 undefined. Contribution of angular motion and gravity to tibial acceleration. EuropepmcOrg n.d.
- [82] Ding Z, Tsang CK, Nolte D, Kedgley AE, Bull AMJ. Improving musculoskeletal model scaling using an anatomical atlas: The importance of gender and anthropometric similarity to quantify joint reaction forces. *IEEE Trans Biomed Eng* 2019;66:3444–56. doi:10.1109/TBME.2019.2905956.
- [83] Prinold JAI, Mazzà C, Di Marco R, Hannah I, Malattia C, Magni-Manzoni S, et al. A Patient-Specific Foot Model for the Estimate of Ankle Joint Forces in Patients with Juvenile Idiopathic Arthritis. *Ann Biomed Eng* 2016;44:247–57. doi:10.1007/s10439-015-1451-z.
- [84] Weygers I, Kok M, Konings M, Hallez H, De Vroey H, Claeys K. Inertial Sensor-Based Lower Limb Joint Kinematics: A Methodological Systematic Review. *Sensors* 2020. doi:10.3390/s20030673.
- [85] Slade P, Habib A, Hicks JL, Delp SL. An open-source and wearable system for measuring 3D human motion in real-time. *IEEE Trans Biomed Eng* 2021;XX:1. doi:10.1101/2021.03.24.436725.
- [86] Al Borno M, O’day J, Ibarra V, Dunne J, Seth A, Habib A, et al. OpenSense: An open-source toolbox for Inertial-Measurement-Unit-based measurement of lower extremity kinematics over long durations. *BioRxiv* 2021:2021.07.01.450788. doi:10.1101/2021.07.01.450788.
- [87] Wouters I, Almonroeder T, Dejarlais B, Laack A, Willson JD, Kernozek TW. Effects of a movement training program on hip and knee joint frontal plane running mechanics. *Int J Sports Phys Ther* 2012;7:637–46.
- [88] Camargo F, Ackermann M, Loss JF, Sacco ICN. Influence of center of pressure estimation errors on 3D inverse dynamics solutions during gait at different velocities. *J Appl Biomech* 2013;29:790–7. doi:10.1123/jab.29.6.790.
- [89] Camomilla V, Cereatti A, Cutti AG, Fantozzi S, Stagni R, Vannozzi G. Methodological factors affecting joint moments estimation in clinical gait analysis: A systematic review. *Biomed Eng Online* 2017;16. doi:10.1186/s12938-017-0396-x.
- [90] Begue J, Caderby T, Peyrot N, Dalleau G. Influence of gait speed on free vertical moment during walking. *J Biomech* 2018;75:186–90. doi:10.1016/j.jbiomech.2018.05.011.
- [91] Holden JP, Cavanagh PR. The free moment of ground reaction in distance running and its changes with pronation. *J Biomech* 1991;24. doi:10.1016/0021-9290(91)90167-L.
- [92] Mundt M, Koeppe A, David S, Witter T, Bamer F, Potthast W, et al. Estimation of Gait Mechanics Based on Simulated and Measured IMU Data Using an Artificial Neural Network. *Front Bioeng Biotechnol* 2020;8:41. doi:10.3389/fbioe.2020.00041.
- [93] Dorschky E, Nitschke M, Seifer AK, van den Bogert AJ, Eskofier BM. Estimation of gait kinematics and kinetics from inertial sensor data using optimal control of musculoskeletal models. *J Biomech* 2019;95:109278.

- doi:10.1016/j.jbiomech.2019.07.022.
- [94] Ancillao A, Tedesco S, Barton J, O’Flynn B. Indirect Measurement of Ground Reaction Forces and Moments by Means of Wearable Inertial Sensors: A Systematic Review. *Sensors* 2018;18:2564. doi:10.3390/s18082564.
- [95] Zioupos P, Currey JD, Casinos A. Tensile fatigue in bone: Are cycles-, or time to failure, or both, important? *J Theor Biol* 2001;210:389–99. doi:10.1006/jtbi.2001.2316.
- [96] OpenSense - Kinematics with IMU Data - OpenSim Documentation - Algemene site n.d. <https://simtk-confluence.stanford.edu/display/OpenSim/OpenSense++Kinematics+with+IMU+Data#OpenSense-KinematicswithIMUData-CustomizingtheOpenSenseWorkflowviaMatlabScriptingmatlabscripting> (accessed February 22, 2021).
- [97] IMU Placer - OpenSim Documentation - Algemene site n.d. <https://simtk-confluence.stanford.edu:8443/display/OpenSim/IMU+Placer> (accessed November 25, 2021).
- [98] How IMU Placer Works - OpenSim Documentation - Algemene site n.d. <https://simtk-confluence.stanford.edu:8443/display/OpenSim/How+IMU+Placer+Works> (accessed November 25, 2021).
- [99] IMU Inverse Kinematics - OpenSim Documentation - Algemene site n.d. <https://simtk-confluence.stanford.edu:8443/display/OpenSim/IMU+Inverse+Kinematics> (accessed November 25, 2021).
- [100] API: OpenSim::IMUInverseKinematicsTool Class Reference n.d. [https://simtk.org/api\\_docs/opensim/api\\_docs/classOpenSim\\_1\\_1IMUInverseKinematicsTool.html](https://simtk.org/api_docs/opensim/api_docs/classOpenSim_1_1IMUInverseKinematicsTool.html) (accessed November 25, 2021).
- [101] How IMU Inverse Kinematics Works - OpenSim Documentation - Algemene site n.d. <https://simtk-confluence.stanford.edu:8443/display/OpenSim/How+IMU+Inverse+Kinematics+Works> (accessed November 25, 2021).



## Appendix

### I – OpenSense: register IMUs to OpenSim model using sensor orientations

For reprocessing IMU data to kinematics, the OpenSense workflow was used, as proposed by [85,86]. This is an extension of OpenSim and is an open-source platform to calculate kinematics from inertial measurement units (IMUs) [96]. Using Xsens software (MVN Analyze, 2020.0.2, Xsens, Enschede, The Netherlands) and OpenSense capabilities through MATLAB scripting (MATLAB R2019b, MathWorks Inc., MA, USA), sensor orientations (quaternions) were obtained from every sensor. Because some jumps were detected in the data, a custom written MATLAB-script was used to first interpolate orientation data at these instances.

Sensor-to-segment registration was performed with the IMU Placer Tool [97,98]. This tool associates the orientation of each sensor with the corresponding segment, which were in this study sternum, pelvis, femurs, tibias, and feet. Each sensor orientation was rotated -90 degrees around the x-axis to match the OpenSim coordinate system. The segment frames for the IMU were identified during a neutral pose, which was collected during each experiment. The IMU Placer Tool also has the option to specify a base IMU and a base heading axis. If a base IMU and heading is specified, OpenSim rotates all orientation data such that the base heading is aligned with the x-axis (forward) in OpenSim. No heading correction was applied in this study, because earlier pilots demonstrated better results when this was not applied.

Inverse kinematics were then calculated with the Inverse Kinematics Tool [99,100]. This tool calculates inverse kinematics based on weighted least squares. The tool minimizes the error between the orientation data of the model and the IMU orientation, i.e.:

$$\min_q \sum_{i \in IMUs} w_i \theta_i^2 \quad (1)$$

Here,  $q$  refers to the joint angles,  $w_i$  refers to the weights for each IMU orientation and  $\theta_i$  is the orientation error expressed as an angle [101].



**II – Proximal versus distal PTA results per runner for 12 km/h at preferred SF****Table 3**

Proximal and distal PTA values per runner for 12 km/h at preferred SF.

| <b>Runner</b> | <b>Proximal PTA (m/s<sup>2</sup>)</b> | <b>Distal PTA (m/s<sup>2</sup>)</b> | <b>p-value</b> |
|---------------|---------------------------------------|-------------------------------------|----------------|
| 1             | 87.0 ± 7.6                            | 71.7 ± 6.3                          | < 0.001        |
| 2             | 61.0 ± 7.3                            | 67.6 ± 5.9                          | < 0.001        |
| 3             | 79.8 ± 5.9                            | 87.8 ± 6.9                          | <0.001         |
| 4             | 85.2 ± 12.6                           | 98.8 ± 12.1                         | <0.001         |
| 5             | 63.0 ± 5.4                            | 77.5 ± 6.8                          | <0.001         |
| 6             | 39.7 ± 6.2                            | 71.5 ± 5.9                          | <0.001         |
| 7             | 88.3 ± 5.3                            | 60.7 ± 3.5                          | <0.001         |
| 8             | 90.3 ± 5.9                            | 87.3 ± 3.8                          | <0.001         |
| 9             | 70.5 ± 7.9                            | 61.2 ± 6.1                          | <0.001         |
| All           | 73.8 ± 17.6                           | 76.0 ± 14.0                         | 0.02           |

Mean ± SD in m/s<sup>2</sup> values for proximal and distal PTA at 12 km/h at preferred SF for every runner and all runners together.



### III – Overview of found Pearson's r for changes in speed and changes in SF for PTA and maximal tibial compression force

**Table 4**

Correlations between speed and all parameters and correlations between SF and all parameters.

| Runner   | Change in speed |        |                        | Change in SF |        |                        |
|----------|-----------------|--------|------------------------|--------------|--------|------------------------|
|          | PTA             |        | $F_{\text{tibia,max}}$ | PTA          |        | $F_{\text{tibia,max}}$ |
|          | Proximal        | Distal |                        | Proximal     | Distal |                        |
| <b>1</b> | 0.8**           | 0.7**  | 0.4**                  | -0.1         | 0.6**  | -0,2                   |
| <b>2</b> | 0.7**           | 0.9**  | -0.7**                 | -0.8**       | -0.8** | 0,5**                  |
| <b>3</b> | 0.8**           | 0.8**  | 0.3**                  | -0.9**       | -0.9** | 0,2*                   |
| <b>4</b> | 0.8**           | 0.9**  | 0.8**                  | 0.1          | 0.3**  | -0,9**                 |
| <b>5</b> | 0.8**           | 0.9**  | 0.8**                  | 0.1          | 0.1    | -0,1                   |
| <b>6</b> | 0.7**           | 0.9**  | 0.6**                  | -0.8**       | -0.6** | -0,5**                 |
| <b>7</b> | 0.7**           | 0.9**  | 0.9**                  | 0.5**        | 0.5**  | 0.0                    |
| <b>8</b> | 0.9**           | 0.9**  | 0.3**                  | -0.5**       | -0.4** | -0,7**                 |
| <b>9</b> | 0.7**           | 0.8**  | 0.7**                  | 0.1          | -0.5** | -0,9**                 |

Response of PTA (proximal and distal) to changes in speed (left part of table) and changes in SF (right part). So, for runner 1, a  $r = 0.8$  between proximal PTA and speed,  $r = 0.7$  between distal PTA and speed and  $r = 0.4$  between  $F_{\text{tibia,max}}$  and PTA. A \* indicates significance at 0.05 level, \*\* indicates significance at 0.01 level.



#### IV – Scatter plots of maximal tibial compression force and PTA for speed

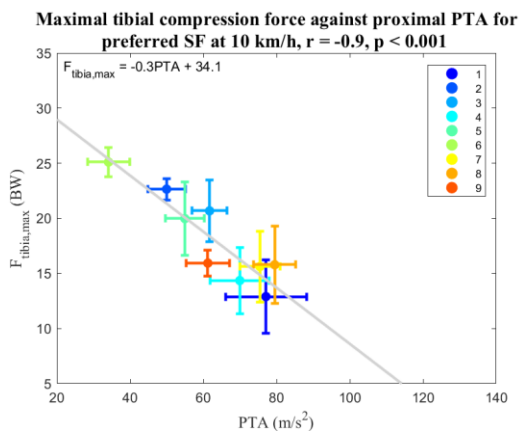


**Fig. 11** Scatter plot of maximal tibial compression force against proximal PTA for 10 km/h at preferred SF.

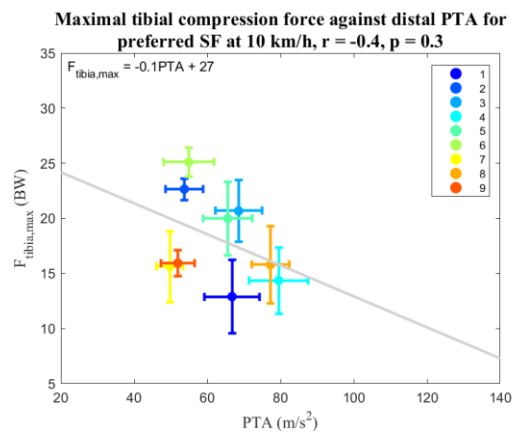


**Fig. 12** Scatter plot of maximal tibial compression force against distal PTA for 10 km/h at preferred SF.

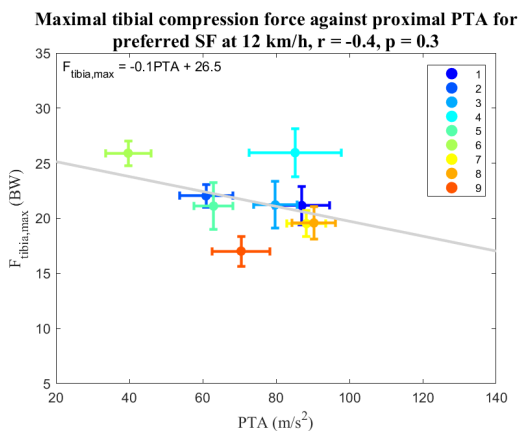


**Fig. 13** Scatter plot of maximal tibial compression force against proximal PTA for 12 km/h at preferred SF.

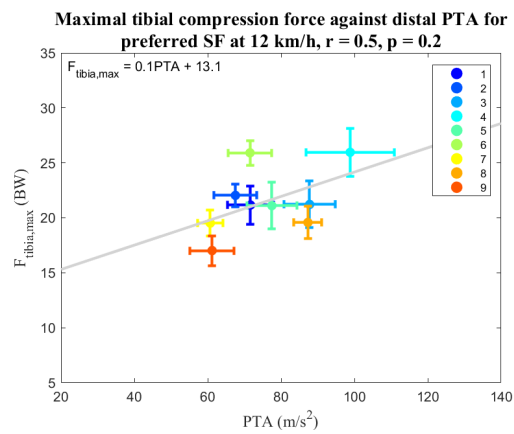


**Fig. 14** Scatter plot of maximal tibial compression force against distal PTA for 12 km/h at preferred SF.

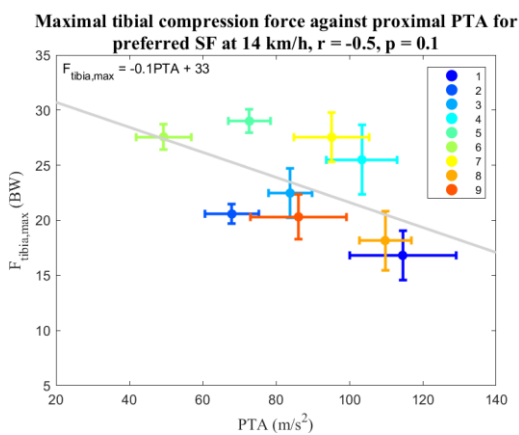


**Fig. 15** Scatter plot of maximal tibial compression force against proximal PTA for 14 km/h at preferred SF.

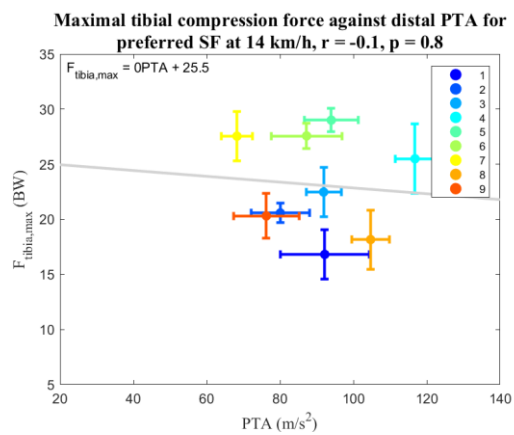


**Fig. 16** Scatter plot of maximal tibial compression force against distal PTA for 14 km/h at preferred SF.



V – Scatter plots of maximal tibial compression force and PTA for SF

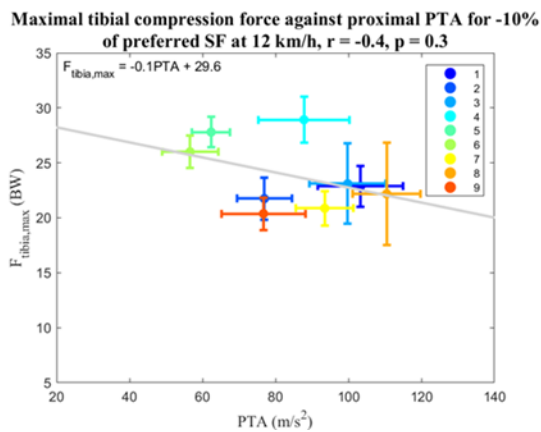


**Fig. 17** Scatter plot of maximal tibial compression force against proximal PTA for -10% of preferred SF.

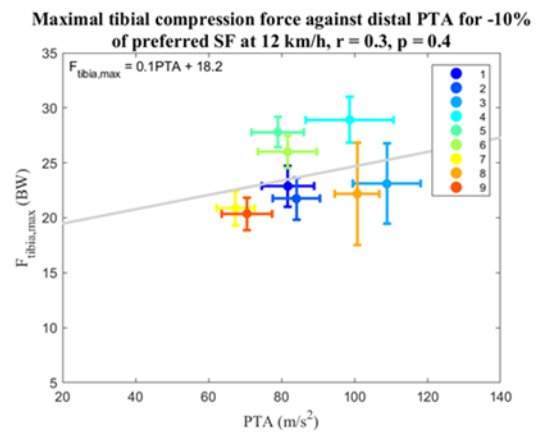


**Fig. 18** Scatter plot of maximal tibial compression force against distal PTA for -10% of preferred SF.

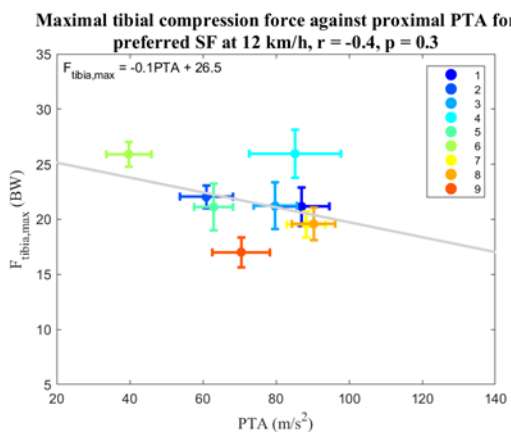


**Fig. 19** Scatter plot of maximal tibial compression force against proximal PTA for 12 km/h at preferred SF.

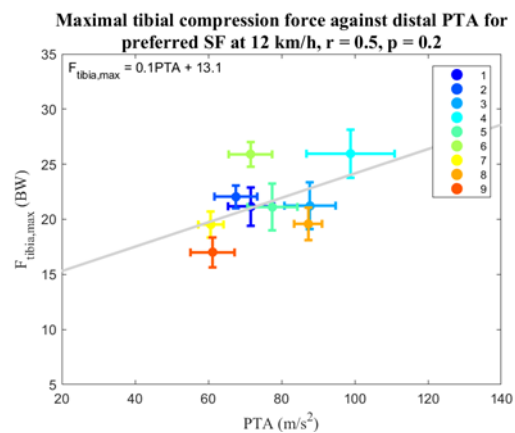


**Fig. 20** Scatter plot of maximal tibial compression force against distal PTA for 12 km/h at preferred SF.

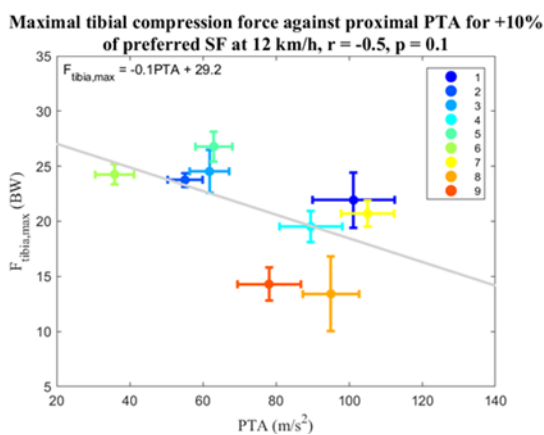


**Fig. 21** Scatter plot of maximal tibial compression force against proximal PTA for +10% of preferred SF.

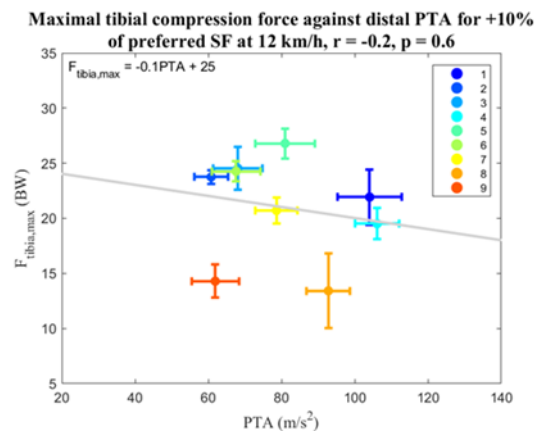


**Fig. 22** Scatter plot of maximal tibial compression force against distal PTA for +10% of preferred SF.



**VI – Relative change in step frequency for every runner****Table 5**

Relative change in step frequency for every runner at 12 km/h.

|          | Measured preferred SF (SPM) | +10% of preferred SF |                     | -10% of preferred SF |                     |
|----------|-----------------------------|----------------------|---------------------|----------------------|---------------------|
|          |                             | Measured (SPM)       | Relative change (%) | Measured (SPM)       | Relative change (%) |
| <b>1</b> | 159                         | 175                  | 10                  | 144                  | -10                 |
| <b>2</b> | 179                         | 198                  | 11                  | 163                  | -9                  |
| <b>3</b> | 167                         | 185                  | 11                  | 151                  | -10                 |
| <b>4</b> | 166                         | 184                  | 11                  | 151                  | -10                 |
| <b>5</b> | 188                         | 204                  | 9                   | 178                  | -5                  |
| <b>6</b> | 187                         | 206                  | 10                  | 177                  | -5                  |
| <b>7</b> | 164                         | 180                  | 10                  | 154                  | -6                  |
| <b>8</b> | 170                         | 187                  | 10                  | 153                  | -10                 |
| <b>9</b> | 172                         | 184                  | 7                   | 161                  | -6                  |

Relative change in SF as measured by an independent researcher. Runners were instructed to run at +10 and -10% of preferred SF.



This page intentionally left blank.

